JAERI-Research
2000-005

ANALYSIS OF CHROMOSOME ABERRATION DATA BY HYBRID-SCALE MODELS

February 2000

Iwiq INDRAWATI* and Shigeru KUMAZAWA

日本原子力研究所
Japan Atomic Energy Research Institute

本レポートは、日本原子力研究所が不定期に公刊している研究報告書です。
入手の問合わせは、日本原子力研究所研究情報部研究情報課（〒319-1195　茨城県那珂郡東海村）あて、お申し越し下さい。なお、このほかに財団法人原子力弘済会資料センター（〒319-1195　茨城県那珂郡東海村日本原子力研究所内）で複写による実費頒布を行っております。

This report is issued irregularly.
Inquiries about availability of the reports should be addressed to Research Information Division, Department of Intellectual Resources, Japan Atomic Energy Research Institute, Tokai-mura, Naka-gun, Ibaraki-ken 〒319-1195, Japan.

編集兼発行　日本原子力研究所

JAERI－Research 2000－005

Analysis of Chromosome Aberration Data by Hybrid-Scale Models

Iwiq INDRAWATI* and Shigeru KUMAZAWA

Nuclear Technology and Education Center
Japan Atomic Energy Research Institute
Honkomagome, Bunkyou-ku, Tokyo

(Received January 14, 2000)

This paper presents a new methodology for analyzing data of chromosome aberrations, which is useful to understand the characteristics of dose-response relationships and to construct the calibration curves for the biological dosimetry. The hybrid scale of linear and logarithmic scales brings a particular plotting paper, where the normal section paper, two types of semi-log papers and the log-log paper are continuously connected. The hybrid-hybrid plotting paper may contain nine kinds of linear relationships, and these are conveniently called hybrid scale models. One can systematically select the best-fit model among the nine models by finding the conditions for a straight line of data points. A biological interpretation is possible with some hybrid-scale models. In this report, the hybrid scale models were applied to separately reported data on chromosome aberrations in human lymphocytes as well as on chromosome breaks in Tradescantia. The results proved that the proposed models fit the data better than the linear-quadratic model, despite the demerit of the increased number of model parameters. We showed that the hybrid-hybrid model (both variables of dose and response using the hybrid scale) provides the best-fit straight lines to be used as the reliable and readable calibration curves of chromosome aberrations.

Keywords: Dose-Response, Linear-Quadratic, Hybrid-Scale, Hybrid-Hybrid Paper, Hybrid Scale Models, Hybrid-Hybrid Model, Dicentrics, Human, Linear Calibration Curve

* Research and Development on Radiation and Nuclear Biomedical Center, National Nuclear Energy Agency, Indonesia

ハイブリッドスケールモデルを用いた染色体異常データの解析

日本原子力研究所国際原子力総合技術センター
Iwiq INDRAWATI*・熊澤　蕃

（2000年1月14日受理）

本報告書は、線量－反応関係に関する特性の理解を深めるとともに、生物学的線量測定に用いる校正曲線の作成に役立てるため、染色体異常データを新たな観点から解析する方法を示す。線形スケールと対数スケールを1つにしたハイブリッドスケールを用いると、通常方眼紙、2種類の片対数方眼紙及び両対数方眼紙を連続に接続した1つの両混成方眼紙が得られる。この両混成方眼紙は9種類の直線状の線量—反応関係が表示できる。これらを便宜的にハイブリッドスケールモデルと呼ぶ。この方眼紙を用いると、プロット点が直線状に並ぶ条件を見つけることによって、9種類の中から観察データに最も適合するモデルを体系的に選択することができる。いくつかのハイブリッドスケールモデルを用いて生物学的な解釈も行える。本報では、ムラサキツユクサの染色体切断並びにヒトリンパ球における染色体異常に関する複数のデータにハイブリッドスケールモデルを適用した。この結果、提案したハイブリッドスケールモデルは、モデルパラメータ数の増加を考慮しても、線形－2次関数モデルに比べてデータ適合性の勝れていることが分った。また、校正曲線は直線グラフとした方がグラフの推定精度を高めたり、使い易くする上で有利である。ハイブリッドハイブリッドモデル（両変数ともハイブリッドスケールを用いる）は検討した染色体異常データのすべてについて最良の直線適合性を示すことが明らかになった。

日本原子力研究所：〒113-0021　東京都文京区本駒込2-28-49
* インドネシア原子力庁 放射線・核生物医学センター 研究開発部門

Contents

1. INTRODUCTION ····· 1

2. THEORY AND METHOD ····· 1

2.1 Linear-quadratic Model ····· 1

2.2 Hybrid Scale Model ····· 2

2.3 Interpretation of Hybrid Scale Models ····· 3

2.4 A General Approach by the Hybrid Scale ····· 5

2.5 Techniques of Fitting Models to Data: Linear-quadratic ····· 6

2.6 Techniques of Fitting Models to Data: Hybrid Scale ····· 7

3. DATA ANALYSIS ····· 9

3.1 X-ray Induced Chromosome Aberrations in Tradescantia (Sax,1940) ····· 9

3.2 X-ray Induced Chromosome Aberrations in Human Blood (Vulpis, et al. 1976) ····· 11

3.3 Chromosome Aberrations in Human Lymphocytes (Edwards, et al., 1979) ····· 12

3.4 Chromosome Aberrations in Human Lymphocytes (Roos and Schmid, 1998) ····· 12

4. DISCUSSION ····· 13

5. CONCLUSIONS ····· 14

ACKNOWLEDGMENTS ····· 14

REFERENCES ····· 15

目　　次

1. はじめに …… 1

2. 理論と方法 …… 1

2.1 直線－2 次式モデル …… 1

2.2 ハイブリッドスケールモデル …… 2

2.3 ハイブリッドスケールモデルの解釈 …… 3

2.4 ハイブリッドスケールによる一般的方法 …… 5

2.5 データへのモデル適合手法：直線－2 次式 …… 6

2.6 データへのモデル適合手法：ハイブリッドスケール …… 7

3. データ解析 …… 9

3.1 ムラサキツユクサにおける X 線誘発染色体異常 (Sax, 1940) …… 9

3.2 ヒト血液における X 線誘発染色体異常 (Vulpis ら, 1976) …… 11

3.3 ヒトリンパ球における染色体異常 (Edwards ら, 1979) …… 12

3.4 ヒトリンパ球における染色体異常 (Roos and Schmid, 1998) …… 12

4. 検討 …… 13

5. 結論 …… 14

謝辞 …… 14

参考文献 …… 15

1. INTRODUCTION

The dose-response relationship concerning ionizing radiation is important as the basis for the reasonable radiation protection. The relationship should be provided explicitly in the range of dose not only above dose limits recommended by the International Commission on Radiological Protection (ICRP) but also below those if possible. The linear-quadratic (L-Q) model has been well established for more than half a century since the 1940s when Sax used the similar approach to fit data for radiation-induced chromosome aberrations [1]. Despite some unsolved issues, it is generally interpreted that the linear and quadratic terms of dose reflect a contribution of single track events and of two-track events, respectively. In the UNSCEAR 1993 Report [2], the L-Q model is presented to be reasonable for the radiobiological mechanisms, via simple mathematical extension of single-hit target theory so as to include multi-track effects made by means of a general polynomial equation. Greinert and Harder [3] interpreted that the linear and quadratic terms of dose represent two different reaction mechanisms of producing exchange-type chromosome aberrations, that is, intratrack and intertrack pairwise lesion interaction.

A different approach may be beneficial to the better understanding of dose-response relationships as well as the improved presentation of the relationships. One of authors has proposed the hybrid-scale (HS) models for dose-response relationships that fit well some data of chromosome aberrations as well as tumors [4, 5]. The HS model was first applied to the cell survival function that reflects the feedback mechanism of repair and recovery effects. The second HS model was the dose-response function that is the product of power function (dominant in lower doses) and exponential function (dominant in higher doses). The third HS model was the general form of dose-response function that is the product of the first and second HS models. However, the HS models should be more thoroughly examined to test the validity in the analysis of chromosome aberrations.

In biological dosimetry by chromosome aberrations, it is important to establish a reliable calibration curve between yield and dose. The HS models might be expected to give a new methodology for constructing an improved calibration curve of chromosome aberrations. We examine for availability of other types of HS models as well as the above-mentioned HS models. As detailed later, other types of HS models are the fourth HS model and the hybrid-hybrid model. The fourth HS model is similar to the first HS model but with the increasing function of dose. The hybrid-hybrid model is equivalent to the straight line on a new type of the section paper [5] for plotting yield against dose, where each of the axes is the hybrid of the logarithmic and linear scales.

This paper presents the formulation of hybrid-scale models, their application to the analysis of chromosome data and the comparison of the results between L-Q models, including the improved types, and HS models.

2. THEORY AND METHOD

2.1 Linear-quadratic model

A generalized linear-quadratic relationship between yield I and dose D has been expressed as follows:

$$I = (\alpha_0 + \alpha_1 D + \alpha_2 D^2)\exp(-\beta_1 D - \beta_2 D^2), \qquad (1)$$

where α_0 is the spontaneous yield, α_1 and α_2 are coefficients for the linear and quadratic terms of dose, and β_1 and β_2 are coefficients for D and D^2 in the probability of cell survival. Their values should be positive in general. Otherwise, such terms should be deleted in general. Equation (1) is the product of F(D), dose-response function without "cell-killing" effect, and S(D), the probability of cell survival,

$$\left.\begin{aligned} I &= F(D)S(D) \\ F(D) &= \alpha_0 + \alpha_1 D + \alpha_2 D^2 \\ S(D) &= \exp\left(-\beta_1 D - \beta_2 D^2\right) \end{aligned}\right\} . \qquad (2)$$

The yield of aberrations, when not significantly contaminated by the cell-killing effect, may be expressed as

$$I = F(D) = \alpha_0 + \alpha_1 D + \alpha_2 D^2 . \qquad (3)$$

The net yield of $I-\alpha_0$ is the following:

$$I_R = F_R(D) = \alpha_1 D + \alpha_2 D^2 . \qquad (4)$$

Putting $\eta=\alpha_2/\alpha_1$, $\xi=\alpha_1^2/\alpha_2$ and $T=\eta D$, and introducing a function of **wiq**(T) = T (1+T), Equation (4) becomes linear in a function of **wiq**(ηD) as follows:

$$I_R = F_R(D) = \xi \,\mathrm{wiq}(\eta D) . \qquad (5)$$

The reciprocal of η has a unit of dose and it means the dose at which the linear term is equal to the quadratic term. The coefficient ξ is dimensionless. Given a biological system of chromosome aberrations, the value of η is almost constant and then the value of **wiq**(ηD) is determined only by each dose. The data plotted as (**wiq**(ηD), I_R) brings a straight line of dose-response, which is convenient to determine the best fit for models in general. The dose-response curve is dominated by the linear term for $\eta D \ll 1$ because then **wiq**(ηD)$\approx\eta$D and by the quadratic term for $\eta D \gg 1$ because then **wiq**(ηD)$\approx(\eta D)^2$. Thus, the value of the scaled dose ηD always shows the dominance between the linear and quadratic components by plotting it in the scale of **wiq**(ηD).

2.2 Hybrid scale model

The linear and logarithmic functions are respectively given by y=x and y=**ln**(x). The sum of both functions defines a hybrid function, which is

$$\mathrm{hyb}(x) = x + \ln(x) . \qquad (6)$$

Figure 1 shows an example of the hybrid function. It approximates the logarithmic function y=**ln**(x) in the range of $x \ll 1$ and becomes asymptotic to the linear function y=x in the range of $x \gg 1$. The hybrid function increases monotonously with the increase of x. Its inverse function denoted as **cyb**(x) increases monotonously by increasing x, as shown in Figure 1. The cyb function approximates the exponential function y=**exp**(x) in the range of $x \ll -1$ and becomes similar to the linear function y=x in the range of $x \gg 1$. The hybrid function and its inverse function are basic mathematical tools to use the HS models. The hybrid function produces a hybrid of the linear scale and the logarithmic

scale as shown in Figure 2. The hybrid scale of x is quite similar to the logarithmic scale for $x \ll 1$, while it approaches the linear scale for $x \gg 1$ (see Figure 2).

A generalized form of dose-response relationship according to the hybrid scale model is expressed by using the conventional functions as follows:

$$I = \left[\alpha_0 + aD^b \exp(cD)\right] S(D), \tag{7}$$

where α_0 is the spontaneous yield, a, b and c are parameters. The probability of cell survival S(D) is defined by the hybrid scale

$$hyb(\rho S) = \delta - \lambda D \quad \text{or} \quad S(D) = \frac{1}{\rho}\mathrm{cyb}(\delta - \lambda D), \tag{8}$$

where S is S(D) and δ is **hyb**(ρ) when S=1 at D=0. Equation (8) is called the first HS model for convenience. In Equation (7), the first term of the right-hand side is the dose-response function without cell-killing effect, which is expressed by the hybrid function as follows:

$$\begin{aligned} F(D) &= \alpha_0 + aD^b \exp(cD) = \alpha_0 + \{(\tau D)\exp(\alpha\tau D)\}^b \\ &= \alpha_0 + \exp[\alpha + \beta\,\mathrm{hyb}(\tau D)] \end{aligned} \tag{9}$$

where α, β and τ are parameters of the HS model.

Putting $I_R = F_R(D) = I - \alpha_0$, Equation (9) becomes linear,

$$\ln(I_R) = \ln\{F_R(D)\} = \alpha + \beta\,\mathrm{hyb}(\tau D). \tag{10}$$

This equation is called the second HS model. The excess incidence or net yield not significantly contaminated by the cell killing effect can be formulated by Equation (10). The parameter α depends on the magnitude of the net yield. The parameter β determines the shape of dose-response function, which is similar to the linear model for β=1 and the quadratic model for β=2 in the range of low doses, $\tau D \ll 1$. The second HS model is the product of the power function and the exponential function. The parameter τ scales the dose at which the net yield should occur in the biological phenomena modeled by a hybrid between power function and exponential function. The larger the value of τ is, the more the net yield exists.

Equation (10) shows that the logarithmic yield of aberrations induced by radiation is proportional to the hybrid function of dose scaled by τ, which approaches **ln**(τD) when $\tau D \ll 1$, and which is close to τD when $\tau D \gg 1$. Equation (8) shows the linear relationship between the hybrid function of survival probability scaled by ρ and dose. Thus, from Equations (8) and (10), the yield of chromosome aberrations is given as the product

$$I = \left[F_R(D) + \alpha_0\right] S(D) = F(D)S(D). \tag{11}$$

Equation (11) or (7) is called the third HS model.

2.3 Interpretation of hybrid scale models

The survival curve for high LET radiation is given as a function, S=**exp**(-λD). Its differential form is

$$\frac{dS}{dD} = -\lambda S \quad \text{or} \quad \frac{d\ln S}{dD} = -\lambda. \tag{12}$$

The second equation gives a straight line on the semi-log paper of (D, **ln**S). The surviving fraction given by Equation (12) means neither repair nor recovery of damaged cells. However, some effect of repair or recovery makes the slope of d**ln**(S)/dD smaller and the curve of surviving fraction has a shoulder on the semi-log plot. The stronger the effect is, the smaller the slope of d**ln**(S)/dD becomes. It is interpreted that the effect of repair or recovery virtually reduces the inactivation constant λ. Suppose the resultant reduction of inactivation constant as given by λ−ρ|dS/dD| instead of λ, the surviving fraction becomes $dS/dD = -(\lambda - \rho|dS/dD|)\,S$, which is also arranged as (1+ρS) dS/dD=−λS, and then

$$\frac{dS}{dD} = -\left(\frac{\lambda}{1+\rho S}\right)S. \tag{13}$$

The value of (1+ρS) is always greater than one and increases with the value of ρ. In turn, the effectiveness of the inactivation constant becomes smaller. The positive value of ρ is interpreted to show the effectiveness of repair or recovery in the cell system. Thus, the surviving fraction in the cell system with repair or recovery is formulated by the inactivation constant λ and the protective factor ρ.

Equation (13) may be transformed as

$$\frac{d}{dD}[\rho S + \ln(\rho S)] = \frac{d\,\mathrm{hyb}(\rho S)}{dD} = -\lambda. \tag{14}$$

The cell system with a function of repair or recovery incorporates the linear term of ρS. Without such a function of repair or recovery, the cell system shows only the logarithmic term of S as shown in Equation (12). Plotting the data of surviving fraction on the hybrid scale by giving ρ, we have a straight line that has a value of **hyb**(ρ) at D=0 if S=1 when D=0. This is the reason to coin the hybrid-scale model for the probability of cell survival in Equation (8).

The hybrid scale model of Equation (8) becomes the linear relationship in very low doses and the exponential relationship in higher doses. The cell surviving fraction where ρS=**ln**(ρS) is the boundary between the linear and exponential relationships. It is called the boundary cell survival, S_B. Putting $D=D_B$ corresponding to S_B, the effectiveness of repair or recovery is significant below the dose of D_B, but insignificant above D_B. The value of **hyb**(ρS) at D=0, **hyb**(ρ), indicates the overall effectiveness of repair or recovery. It likely corresponds to quasi-threshold dose, D_0, or extrapolation number, n.

Next, we consider the model of dose-response relationship without cell-killing effect. The net yield (subtracting the control) is sometimes expressed as the power function of $I_R=aD^b$. However, on increasing dose, the yield will be accelerated more depending on the magnitude of dose. One of accelerating terms is the multiplication by **exp**(cD). Then the net yield can be of a form $I_R=aD^b$**exp**(cD). This corresponds to Equation (9) or (10) that has a form of **ln**(I_R)=α+β{**ln**(τD)+τD}=α+β**hyb**(τD). The equation is linear in terms of α and β for a given value of τ, when the hybrid scale is introduced. Without the accelerating effect of yield, it has a form of **ln**(I_R)= α+β**ln**D that is the power function.

With the strong effect of the acceleration, it has a form of $\mathbf{ln}(I_R)= \alpha+\beta D$ that is the exponential function. The form of the hybrid scale model of dose-response relationship is more flexible to fit data than that of the linear-quadratic model as far as we should consider the multi-track effects and other complex situations of biological phenomena.

The derivative $d\mathbf{ln}(I_R)/dD$ gives the relative increment of the net yield associated with the increment of dose. Its reciprocal, $dD/d\mathbf{ln}(I_R)$, means the amount of dose required for the unit relative increase of the net yield. Without an acceleration of the yield, $dD/d\mathbf{ln}(I_R)=D/\beta$. When the dose becomes considerably higher, the acceleration of the yield can be more significant because of a deficiency in repair or recover. The deficiency likely tends to reduce the dose increment required for the unit relative increase by depending on the magnitude of $dD/d\mathbf{ln}(I_R)$. Replacing $1/\beta$ by $1/\beta-\tau dD/d\mathbf{ln}(I_R)$, one obtains $dD/d\mathbf{ln}(I_R)=D/\beta/(1+\tau D)$. This is expressed as $d\{\tau D+\mathbf{ln}(\tau D)\}/d\mathbf{ln}(I_R)=d\mathbf{hyb}(\tau D)/d\mathbf{ln}(I_R)=1/\beta$. The logarithmic increment, $\Delta\mathbf{ln}(I_R)$, of the yield is considered only when the change of the yield seems to be almost due to the multiplicative interactions.

2.4 A general approach by the hybrid scale

One of the most important approaches in constructing the dose-response relationship is to linearize observed data that would not otherwise fall on a straight line. The reasonable linearization of dose-response relationships can bring a reliable fit of models to data, including possible extrapolation in the range of low doses. For that purpose, the logarithmic scale is often used. The use of the hybrid scale, however, dramatically extends the possibility of the linearization. This is due to the unification of the linear scale and the logarithmic scale.

The hybrid scale extends the conventional section papers not only in the variety of section papers as shown in Figure 3, but also in the unification of the whole papers as a hybrid-hybrid paper as shown in Figure 4. The hybrid scale consists of typically three regions, the logarithmic, the hybrid and the linear region. The introduction of the hybrid scale to both vertical and horizontal axes displays nine kinds of section papers shown in Figure 3. Five section papers interfacing conventional papers are new. These are two semi-hybrid papers of (x, **hyb**(y)) and (**hyb**(x), y), two log-hybrid papers of (**ln**(x), **hyb**(y)) and (**hyb**(x), **ln**(y)), and one hybrid-hybrid paper of (**hyb**(x), **hyb**(y)).

Among HS papers, the hybrid-hybrid paper is special to provide the concept of unifying nine section papers. As may from Figure 4, the center region of the hybrid-hybrid paper continuously interfaces its surrounding regions. Thus, the hybrid-hybrid paper unifies four popular section papers that have been used separately. The unification provides the flexibility for expressing the complex relationships between stimuli and responses in biological phenomena that might show diverse dependence from the additive to the multiplicative due to some possible control mechanisms.

The first HS model for cell survival uses the right side region of the hybrid-hybrid paper as a decreasing straight line. The second HS model of dose-response relationship uses the lower side region of the hybrid-hybrid paper as an increasing straight line. The fourth HS model is introduced as an increasing straight line on the right side region of the hybrid-hybrid paper,

$$\mathrm{hyb}(vY) = a + bD \quad \text{or} \quad Y = \frac{1}{v}\mathrm{cyb}(a + bD). \tag{15}$$

$$\mathrm{hyb}(vY) = a + bD \quad \text{or} \quad Y = \frac{1}{v}\mathrm{cyb}(a + bD). \tag{15}$$

This will be applied to some data later. The hybrid-hybrid model is introduced as an increasing straight line on the hybrid-hybrid paper as follows:

$$\mathrm{hyb}(vY) = \alpha + \beta\,\mathrm{hyb}(vD) \quad \text{or} \quad Y = \frac{1}{v}\mathrm{cyb}[\alpha + \beta\,\mathrm{hyb}(vD)]. \tag{16}$$

2.5 Techniques of fitting models to data: Linear-quadratic

The L-Q models of Equations (3) and (4) are linear with respect to parameters. These are solved easily, for example, by the function LINEST of the MS-EXCEL. The principle is to minimize the sum, $\Sigma\varepsilon_j^2$, of squared residual errors between data and model estimates, where data is a set of $\{D_j, I_j \mid j=1, n\}$. The yield I_j is calculated as M_j/N_j where N_j is the number of cells scored, M_j is the number of chromosome aberrations. The variance of M_j is $N_j\times(M_j/N_j)\times(1-M_j/N_j)$ by the binomial distribution or M_j by Poisson distribution. The statistical error SE_j of the yield is calculated as the root square of M_j/N_j $(1-M_j/N_j)/N_j$ or M_j/N_j^2, respectively. The residual error is calculated from the following equation.

$$I_j = \alpha_0 + \alpha_1 D_j + \alpha_2 D_j^{\,2} + \varepsilon_j = \hat{I}_j + \varepsilon_j. \tag{17}$$

To use Equation (4), the intercept α_0 is zero.

The weighted least squares equation is to minimize $\Sigma\varepsilon_j^2/SE_j^2$. Putting $w_j=1/SE_j^2$, the equation is given as follows:

$$w_j I_j = \alpha_0(w_j) + \alpha_1(w_j D_j) + \alpha_2(w_j D_j^{\,2}) + w_j\varepsilon_j. \tag{18}$$

Equation (18) is solved by the function LINEST.

For the data ranging several orders of magnitude, the sum of squared relative residual errors is often minimized. The minimization of $\Sigma(\varepsilon_j/I_{R,j})^2$ by the observations, as seen in [6], is somewhat an unstable method because of dependence on the variation of data. The minimization of $\Sigma(\varepsilon_j/\hat{I}_{R,j})^2$ by the estimations is more stable because of no variation in the model calculation. Both are solved by the nonlinear least squares method, for example, by the tool SOLVER of the MS-EXCEL.

In NCRP Report No.60, the following type of equation is used to estimate the parameters of the L-Q model [7].

$$\ln(I_{R,j}) = \ln(\alpha_1 D_j + \alpha_2 D_j^{\,2}) + \varepsilon_j, \tag{19}$$

To estimate the value of α_0, the equation is replaced by

$$\ln(I_j - \alpha_0) = \ln(\alpha_1 D_j + \alpha_2 D_j^{\,2}) + \varepsilon_j. \tag{19'}$$

Equation (19) provides the similar estimates of parameters to that by minimizing the sum of squared relative residual errors.

The linear scale in vertical axis is inclined to emphasize large positive values but to squeeze small positive values for the data ranging several orders of magnitude. The larger contribution of increasing squared-errors in large values gives rise to a tendency to

(17) in the linear scale and Equation (19) in the logarithmic scale show this dilemma for the yield with the variation of additive and multiplicative effects. To solve the dilemma, especially for the data ranging several orders of magnitude, the hybrid scale is applied as

$$\mathrm{hyb}[vI_{R,j}] = \mathrm{cyb}[v(\alpha_1 D_j + \alpha_2 D_j^{\,2})] + \varepsilon_j. \tag{20}$$

The parameters are estimated by the tool SOLVER of the MS-EXCEL. The value of v is obtained from fitting the hybrid-hybrid model.

For the L-Q model of cell survival, Equation (2) is solved by the tool SOLVER. The following equation is solved by the function LINEST.

$$\ln(S_j) = -\beta_1 D_j - \beta_2 D_j^{\,2} + \varepsilon_j. \tag{21}$$

Equation (2) is in the linear scale and Equation (21) is in the logarithmic scale for S. The same dilemma of the scale is considered for estimating the parameters.

The general form of linear-quadratic model might be solved by the tool SOLVER, after selecting the initial values of parameters. The initial values of parameters are obtained from Equation (17) or (18) of the dose-response relationship and Equation (21) of cell survival by using the linear least squares method. The weighted nonlinear least squares method is more appropriate, especially weighted by the reciprocal of the variance associated with each of data.

2.6 Techniques of fitting models to data: Hybrid scale

The second HS model of Equation (10) is solved by the function LINEST in terms of a_0, a_1 and a_2 as follows:

$$\ln(I_{R,j}) = \alpha + \beta\,\mathrm{hyb}(\tau D_j) + \varepsilon_j = a_0 + a_1 D_j + a_2 \ln(D_j) + \varepsilon_j. \tag{22}$$

The parameters of α, β and τ are calculated from the estimation of a_0, a_1 and a_2 by

$$\hat{\alpha} = \hat{a}_0 - \hat{a}_2 \ln\frac{\hat{a}_1}{\hat{a}_2}, \quad \hat{\beta} = \hat{a}_2, \quad \hat{\tau} = \frac{\hat{a}_1}{\hat{a}_2}. \tag{23}$$

The statistical error of the net yield is the root square of summing the variance of the spontaneous yield and a given yield. Putting it as s_j, the logarithmic weight is the root square of $w_j = 2/\ln\{(I_{R,j}+s_j)/(I_{R,j}-s_j)\}$. The weighted least squares equation is linearly solved in terms of a_0, a_1 and a_2 as follows:

$$w_j \ln(I_{R,j}) = a_0 w_j + a_1 w_j D_j + a_2 w_j \ln(D_j) + w_j \varepsilon_j. \tag{24}$$

The logarithmic form of the yield not subtracted by the background is

$$\ln(I_j) = \ln[\alpha_0 + aD_j^{\,b}\exp(cD_j)] + \varepsilon_j. \tag{25}$$

The parameters are solved by the tool SOLVER of the MS-EXCEL. However, to attain the best fit in low doses, it should be replaced by

$$\ln(I_j - \alpha_0) = \alpha + \beta\,\mathrm{hyb}(\tau D_j) + \varepsilon_j. \tag{25'}$$

$$\ln(I_j - \alpha_0) = \alpha + \beta \mathrm{hyb}(\tau D_j) + \varepsilon_j . \qquad (25')$$

The linear form of the net yield for the second HS model of Equation (9) is solved by the tool SOLVER as follows:

$$I_{R,j} = aD_j^{\ b} \exp(cD_j) + \varepsilon_j = (\tau D_j)^{\beta} \exp(\alpha\beta\tau D_j) + \varepsilon_j . \qquad (26)$$

Equation (26) can be weighted by the reciprocal of the variance associated with the net yield. Minimizing the sum of squared relative residual errors by the observation or the estimation provides the estimation of parameters similar to that by the logarithmic form of the yield in Equation (25) or (25'). Adding the background term of α_0 to Equation (26), the model of the yield I_j is estimated.

The hybrid scale form of the net yield for the second HS model is expressed in general as follows:

$$\mathrm{hyb}\left[v(I_j - \alpha_0)\right] = \alpha + \beta \mathrm{hyb}(\tau_1 D_j) + \varepsilon_j . \qquad (27)$$

This form of the model is solved by the tool SOLVER, with or without the weight of the reciprocal of the variance associated with the net yield. The statistical errors are the upper error bar of hyb[v(I_j+s_j)]–hyb[vI_j] and the lower error bar of hyb[vI_j] – hyb[v(I_j–s_j)]. The weight is the square of 2/(hyb[v(I_j+s_j)] – hyb[v(I_j–s_j)]).

For the hybrid scale model of cell survival, Equation (8) is solved by the tool SOVLER, that is

$$S_j = \frac{1}{\rho}\mathrm{cyb}\left[\mathrm{hyb}(\rho) - \lambda D_j\right] + \varepsilon_j . \qquad (28)$$

The following linear equation provides the initial value of parameters ρ_0 and λ_0.

$$\left.\begin{aligned} D_j &= a_1(1 - S_j) + a_2 \ln(S_j) + \varepsilon_j \\ \rho_0 &= -\frac{\hat{a}_1}{\hat{a}_2}\ ,\ \lambda_0 = -\frac{1}{\hat{a}_2} \end{aligned}\right\} . \qquad (29)$$

Equation (28) is the linear form of surviving fractions. The logarithmic form of surviving fractions is given by

$$\ln(S_j) = \rho - \mathrm{cyb}\left[\mathrm{hyb}(\rho) - \lambda D_j\right] - \lambda D_j + \varepsilon_j . \qquad (30)$$

The linear scale squeezes data plots in the range of smaller surviving fractions. On the other hand, the logarithmic scale squeezes those close to the survival of one. However, the hybrid scale does not squeeze data plots in the whole range of surviving fractions. This is given in Equation (8) and is solved by using the tool SOLVER, that is

$$\mathrm{hyb}(\rho S_j) = \mathrm{hyb}(\rho) - \lambda D_j + \varepsilon_j . \qquad (31)$$

The equation might be weighted by the reciprocal of the variance associated with survivals. However, data to which Equation (31) with a proper value of ρ is applicable can fall on a straight line.

In Equation (9) the hybrid scale model should have the positive value for all of a, b and c. Putting c=0, Equation (9) is the power function model. There are three ways of

applying the power function model to data: Data on the logarithmic scale is solved by the function LINEST and data on the linear and hybrid scales are solved by the tool SOLVER. There is a possibility for the case of $c<0$. Then Equation (9) means that the yield follows the exponential function of cell survival as well as the power function of dose-response function.

3. DATA ANALYSIS

Several reported data of chromosome aberrations and the related endpoints are used to examine the validity of selecting and applying models of dose-response relationships. Data to be analyzed are classical ones [8] and those about human lymphocytes [9]-[11]. The classical data are useful for understanding the fundamental characteristics of dose-response relationships. The human lymphocyte data are suitable for the purpose of low-dose risk assessment as well as biological dosimetry.

3.1 X-ray induced chromosome aberrations in Tradescantia *(Sax, 1940) [8]*

The early studies on X-ray induced mutation rate in Drosophila, were reported to show linearity. Late in 1930s, there appeared some studies on both Drosophila and Tradescantia where the relation between X-ray dose and chromosome aberrations was not linear. Sax proved that the frequency of chromosome aberrations increased as the square of the dose given in a constant time, while the previous studies reported that it increased as the 3/2 power of the dose given in a constant dose rate. Table 1 shows his data of chromosome aberrations induced by the X-ray at the resting stage in Tradescantia, which seems to increase as the square of the dose. Sax obtained the best fit of the relation as $B = (D/1.07)^2$, by plotting the data on a log-log paper, where B is the percent breaks of chromosome and D the dose in Gray (assumed 1 Gy = 100 r). His result was based on the theory that the frequency of dicentrics and rings, due to two breaks of chromosome, should increase as the square of the dose.

The percent breaks, if they increase as the square of the dose, fall on a straight line when the data on the logarithmic scale are plotted against the dose on the logarithmic scale. They also fall on a straight line when the data on the linear scale are plotted against the square of the dose. Figure 5 shows these two types of the plots. The left panel is the log-log plot which is the same as Sax's. The right panel is the quadratic-linear plot of (D^2, B) to emphasize the characteristics of the quadratic function. The solid straight line on each panel is the best fit of the power function model to the data on the log-scale with the weight of statistical errors of the percent breaks. This is the same as Sax's result in Table 1. Without the weight, however, there is a difference in the best fit between the linear (dotted line) and the logarithmic scale (broken line). The broken line fits the data in lower doses well (see left panel) but deviates from the data in higher doses (see right panel). On the other hand, the dotted line shows the trend to fit the data to the contrary. This shows the dilemma between the linear and the logarithmic scale in the model fitting. In the case of Sax's data, the solid line fits the whole data best among the three methods for applying the power function model.

The hybrid scale provides another type of linear relationship between dose and percent breaks transformed by the hybrid function. Plotting the yield on the linear scale as points (D,B) brings the downward convex arrays of the data. Plotting the yield on the log scale as points (D, ln[B]) brings the upward convex arrays of the data. These lead to the

possibility of applying the hybrid scale to plot as points (D, hyb[νB]). The plot on the semi-hybrid paper as (D, hyb[νB]) approaches that on the semi-log paper of (D, ln[B]) when $\nu B \ll 1$, and that on the normal section paper of (D, B) when $\nu B \gg 1$. Estimating the value of ν as 0.318 by the nonlinear least squares method, the data (◇) plotted on the semi-hybrid paper fall on the solid straight line, given as hyb[0.318B] = -3.76 + 2.44D, in Figure 6. This is the fourth HS model of dose-response relationship. The background percent breaks of dicentrics and rings in Tradescantia is estimated to be 0.072% per chromosome because B=0.072 at D=0 Gy.

The broken curve in Figure 6 represents the quadratic model of $B=(D/1.08)^2$, fitted to the data on the semi-hybrid paper. This is almost the same as Sax's result in Table 1 and the solid straight line in Figure 5 and fits the whole of the data points almost within the error bar. In Figure 6, however, the fit of solid straight line to the whole data points is clearly better than that of the broken curve. Consequently, it shows that the fourth HS model provides the best fit to the whole of data points among all types of models applied here.

The quadratic model predicts more breaks above the highest observed dose than the fourth HS model in Figure 6. The fourth HS model approaches the linear model at higher doses. If there is any moderate reduction in the increase of the percent breaks due to the cell killing effect or the saturation, such a feature of the fourth HS model is particularly suitable for a good fit to the data.

Sax also showed that the one-hit and two-hit chromatid aberrations induced at prophase were almost linear with the dose and the square of the dose, respectively. His data and the estimated models are given in Table 2. We consider the applicability of the hybrid-hybrid model to these data. The problem is to find the straight line that fits best to the data plotted on the hybrid-hybrid paper as points of (hyb[τD], hyb[νB]). Figure 7 shows hybrid-hybrid plots of the percent chromatid breaks of one-hit (left panel) and two-hit (right panel), the positive values of τ and ν being selected so that the whole data should lie on a straight line. Both panels show good fit of the hybrid-hybrid model to each of the data. All data on the left panel are positive for both axes, and the values of hyb(τD) are especially very large. This is consistent with the linear relation between dose and one-hit chromatid breaks. On the other hand, some data on the right panel are negative for the vertical hybrid scale. This reflects the quadratic relation between dose and two-hit chromatid breaks. Thus, the hybrid-hybrid plot of the data provides a straight array of points for the quadratic case as well as for the linear case.

The total percent of one-hit and two-hit chromatid aberrations was reported to vary with the 3/2 power of the dose by Sax, which is $B = (D/0.37)^{1.5}$. This is the solid straight line on the left panel of the log-log paper in Figure 8. It shows the applicability of the power function model to the dose-response relationship to the data. Replacing the log scale with the hybrid scale for the dose, we have another straight line fitted to the whole of the data as shown on the right panel of Figure 8. The solid straight line represents the second HS model given in Equation (10). As seen in the figure, the second HS model fits the whole of the data better than Sax's power function model. The second HS model also fits each of the whole data of one-hit and two-hit chromatid breaks shown in Table 2. Therefore, the second HS model is applicable to these data.

The total chromatid breaks obtained from Table 2 is also fitted by the L-Q model because each type of the breaks is presumably varying as a function of the dose and the

square of the dose. The left panel in Figure 9 shows the straight line of L-Q model by plotting the data as points of ($\eta D(1+\eta D)$, B), where η is the reciprocal of the boundary dose at which the linear component is equal to the quadratic component. The left panel shows that the whole data is fitted well by the L-Q model (solid straight line). Thus, the L-Q model provides the straight line of best fit to the data on the linear scale. Plotting the same data on the hybrid scale, we have another straight line shown on the right panel in Figure 9. This solid straight line of the hybrid-hybrid model fits the whole data sufficiently. The fitting quality of the hybrid-hybrid model is similar to that of the second HS (dotted curve) and L-Q (broken curve) models in the range of the reported data. The hybrid-hybrid model, however, extrapolates larger values below the reported doses and smaller values above the reported doses than the second HS and L-Q models.

The above analysis shows the applicability of the hybrid scale models to the data given in Tables 1 and 2. At the same time, the characteristics of the hybrid scale models becomes clear by comparing them with the power function and L-Q models and by examining several methods of fitting these models. However, for the risk assessment methodology for low dose radiation, it is important that the possible models should apply to the human chromosome data.

3.2 X-ray induced chromosome aberrations in human blood *(Vulpis, et al., 1976) [9]*

For the purpose of biological dosimetry, Vulpis et al. discussed about the construction of the calibration curves based on the well-established procedures. They used peripheral blood of two healthy male donors, 35 and 39 years old. Table 3 shows their data. They applied the linear model to fit the yield of chromosome aberrations to the seven data below 0.6 Gy and the L-Q model to the whole data including the previously obtained data from 1 to 4 Gy (Vulpis, 1974). Figure 10 is the combined data of the yield of dicentrics plotted on the log-log paper.

We applied the hybrid-hybrid model (solid line in Figure 10) to fit the combined data that extend over the wide range of doses. The solid line fits the data over the whole range of doses well. For comparison, the L-Q (dotted line) and HS (broken line) models are shown in the graph. This L-Q model can be actually called the hybrid-scaled L-Q model. The estimation of parameters minimizes the sum of the squared errors of the yield on the hybrid scale of hyb(νY) where Y is the yield and ν is about 1.28 per unit of yield. The hybrid-scaled L-Q model fits the whole data well but is less fit to the data than the hybrid-hybrid model, while it fits the whole data better than the L-Q model with weight.

The HS model in Figure 10 is the second type of models, which does not contain the term of cell killing or saturation effect. The second HS model fits the whole data almost to the same degree as the hybrid-hybrid model but tends to deviate from the data above the second largest dose. The third HS model provides a better fit to the whole data because of including the term of cell killing or saturation effect. The combined data given in Table 3 does not extend enough to show the explicit decrease of the yield due to the cell killing or saturation effect. Therefore, the estimation of parameters is not reliable for the term of cell killing or saturation. For the construction of calibration curve, the hybrid-hybrid model is more convenient than the third HS model if the curve of the yield does not appear to be upward convex. However, the second HS model is easier to use than the hybrid-hybrid model. The second HS model is better to construct the calibration

curve than the hybrid-hybrid model as far as the effect of cell killing or saturation is negligible.

Figure 11 shows the calibration curve of the whole data in Table 3, which is presented as the straight line on the hybrid-hybrid paper. The straight line estimated by the hybrid-hybrid (HH) model is hyb(1.276Y)=-3.3774+0.9312hyb(1.135D). To estimate the dose based on the calibration curve, we can use the following equation.

$$Y = \frac{1000}{1.276}\mathrm{cyb}[-3.3774 + 0.9312\,\mathrm{hyb}(1.135D)] \quad (\mathrm{mGy})$$

3.3 Chromosome aberrations in human lymphocytes *(Edwards, et al., 1979) [10]*

To study the validity of Poisson statistics in the observation of chromosome aberrations, Edwards et al. published data on the distribution of dicentrics and acentrics observed in human lymphocytes, cultured for 48 h after irradiation by X-rays, cobalt-60 and neutrons. We analyzed two cases of their dicentric data to examine the applicability of hybrid scale models. Table 4 shows the case of 250kVp X-rays at a high dose rate of 1 Gy/min and Table 5 the other case of ^{60}Co gamma rays at a dose rate of 0.5 Gy/min. The yields of dicentrics induced by X-ray and cobalt-60 are plotted on the log-log paper in Figure 12, respectively, as left and right panels. Four curves on each panel represent the best fit in each of the weighted L-Q (broken line), hybrid-scaled L-Q (dot-dot-dashed line), second HS (dotted line) and hybrid-hybrid (solid line) models. In the case of X-ray (left panel), four curves fit the data over the whole range of doses well but the solid curve fits the data best among them. In the case of cobalt-60 (right panel), we also see the similar characteristics.

Figure 13 shows the calibration curves of the yields for X-ray (left panel) and cobalt-60 (right panel), drawn on the hybrid-hybrid paper. Each of the straight lines, estimated by the hybrid-hybrid model, shows a good linearity over the whole range of doses. These are hyb(0.642Y) = −2.1569+1.1317hyb(0.449D) for X-ray and hyb(0.248Y) = −1.7147+1.4656hyb(0.167D) for cobalt-60. To estimate the dose based on the calibration curves, we can use respectively the following equations for X-ray and cobalt-60.

$$Y = \frac{1000}{0.642}\mathrm{cyb}[-2.1569 + 1.1317\,\mathrm{hyb}(0.449D)] \quad (\mathrm{mGy})$$

$$Y = \frac{1000}{0.248}\mathrm{cyb}[-1.7147 + 1.4656\,\mathrm{hyb}(0.167D)] \quad (\mathrm{mGy})$$

3.4 Chromosome aberrations in human lymphocytes *(Roos and Schmid, 1998) [11]*

Roos and Schmid (1998) examined the frequency of chromosome aberrations induced by 5.4 keV X-rays. They found a linear-quadratic dose-response for dicentrics and almost a Poisson statistics in the intercellular distribution of dicentrics. Table 6 shows their data. Being plotted on the log-log paper, the array of points is slightly downward convex as shown on left panel in Figure 14. All the lines for the weighted L-Q (broken line), hybrid-scaled L-Q (dot-dashed line), second HS (dotted line) and hybrid-hybrid (solid line) models appear to fit the whole data fairly well. However, on the normal section paper

(right panel in Figure 14), array of points is more downward convex and slightly deviates from the dashed curve of WLQ. This result is quite similar to those of human data shown before.

Figure 15 shows the calibration curves of the yields for 5.4keV X-ray, presented as the straight line on the hybrid-hybrid paper. This straight line of the hybrid-hybrid model, hyb(0.00386Y) = –6.7217+ 1.1281 hyb(0.432D), fits the whole data completely. The straight line is. To estimate the dose based on the calibration curve, we can use the following equation.

$$Y = \frac{1000}{0.00386}\mathrm{cyb}[-6.7217 + 1.1281\,\mathrm{hyb}(0.432D)] \quad (\mathrm{mGy})$$

4. DISCUSSION

The model for dose-response relationships should be selected depending on the objective. To study the characteristics of the relationship, we should examine each of factors affecting the relationship separately so that we should establish the theory of biological effects. For the biological dosimetry using chromosome aberrations, we should find a reliable relationship between dose and yield, which is estimated by a practical model to be used easily. It is important to know the effects, for example, cell killing or saturation, for the purpose of the calibration curve.

Norman and Sasaki [12] reported the yield of chromosome-exchange aberrations produced by X-rays in human lymphocytes. The mean energy of photon is 1.9 MeV. The dose rate ranges from 1 to 2 Gy/min. They proved that the probability of inducing a dicentric of chromosome is proportional to its length in the interphase nucleus. They also proved that the number of dicentrics and centric rings per cell would be limited primarily by the number of centromeres. We use their dicentric data, shown in Table 7, to examine the effect of cell killing or saturation.

Figure 16 shows the data plotted on the log-log paper (left panel) and on the normal section paper (right panel). The broken, dotted and solid curves represent respectively the best fit of the weighted L-Q model, second HS model and hybrid-hybrid model. The broken and dotted curves deviate clearly from the data points. Calculating the survival fractions by the weighted L-Q and second HS models, we obtain two survival curves relating to the weighted L-Q (△) and second HS (◇) models, shown on left panel in Figure 17. According to Equations (2) and (11), the weighted L-Q and second HS models multiplied by the corresponding cell killing effect provide respectively the upward convex curves of the broken and dotted lines, shown on right panel in Figure 17. Fitting the models to the data by Equation (1) and (7) brings the better fit for each of the models. These fittings are almost the same as that of the hybrid-hybrid model, except for the range of dose below 1 Gy.

Figure 18 shows the yields of the dicentrics falling on a straight line of the hybrid-hybrid model over the whole range of doses 0.5 to 20 Gy. The data of Norman and Sasaki shows the strong effect of cell killing or probably saturation. However, the hybrid-hybrid model also provides the straight line of the calibration curve. The straight line is given by hyb(0.139Y) = 10.3808+ 2.0911 hyb(0.000634D). The following equation provides the dose based on the calibration curve.

$$Y=\frac{1000}{0.139}\mathrm{cyb}[10.3808+2.0911\mathrm{hyb}(0.000634D)] \quad (\mathrm{mGy})$$

5. CONCLUSIONS

The data of chromosome aberrations were analyzed to examine the characteristics of dose-response relationships and the applicability of hybrid scale models for constructing the calibration curves of chromosome aberrations. We used the data of chromosome and chromatid breaks (Sax, 1940) for the start of the study. The fourth hybrid scale model and the hybrid-hybrid model are confirmed to be more applicable than the conventional models. The second hybrid scale model showed applicability to the data of the chromatid breaks. Five data sets of dicentric chromosome aberrations from four papers were fitted best by the hybrid-hybrid model that provides the straight line for the calibration curves over the wide range of doses. Some of the data showed the strong effect of the saturation like a cell killing effect. However, the hybrid-hybrid model provided a sufficiently fitting straight line as the calibration curves. In conclusion, this paper proved that the hybrid-hybrid model is applicable to the analysis of chromosome aberrations.

ACKNOWLEDGMENTS

The authors wish to acknowledge Dr. Y. Murao, Director of the Nuclear Technology and Education Center (NuTEC) for providing the chance of the study, Dr. I. Hayata, Director, Division of Radiobiology and Biodosimetry, National Institute of Radiological Sciences for advising us at the beginning of the study, Drs. M. Saeki and H. Shiraishi, NuTEC, for the peer review, and, Mr. S. Suga and others in the Tokai Education Center for giving advise and encouraging the study.

REFERENCES

[1] Committee on the Biological Effects of Ionizing Radiations. Health effects of exposure to low levels of ionizing radiation- BEIR V (Washington: National Academy Press) (1990).

[2] United Nations Scientific Committee on the Effects of Atomic Radiation. Report of the Scientific Committee on the Effects of Atomic Radiation. Annex F, General Assembly of Official Records, 1993, United Nations, New York.

[3] Greinert, R. and Harder, D. Biophysical analysis of the dose-dependent overdispersion and the restricted linear energy transfer dependence expressed in dicentric chromosome data from alpha-irradiated human lymphocytes. Radiat. Environ. Biophys., 36, 89-95 (1997).

[4] Kumazawa, S. Some hybrid models applicable to dose-response relationships. Proc. Int. Conf. on Radiation Effects and Protection, March 18-20, 1992, Mito, held by Japan Atomic Energy Research Institute. 260-266 (1992).

[5] Kumazawa, S. A hybrid-scale theory to be applied in health risk assessment. Comparative Evaluation of Environmental Toxicants. － Health Effects of Environmental Toxicants Derived from Advanced technologies, January 28-30, 1998, Chiba, held by National Institute of Radiological Sciences. 177-190 (1998).

[6] Foray, N., Badie, C., Alsbeih, G., Fertil, B., and Malaise, E.P. A new model describing the curves for repair of both DNA double-strand breaks and Chromosome damage. Radiat. Res., 146, 53-60 (1996).

[7] National Council on Radiation Protection and Measurements. Influence of dose and its distribution in time on dose-response relationships for low-LET radiations. NCRP Report No.64 (1980).

[8] Sax, K. An analysis of x-ray induced chromosomal aberrations in Tradenscantia. Genetics, 25, 41-68 (1940).

[9] Vulpis, N., Panetta, G. and Tognacci, L. Radiation-induced chromosome aberrations in radiological protection: Dose-response curves at low dose-levels. Int. J. Radiat. Biol., 29, 595-600 (1976).

[10] Edwards, A.A., Lloyd, D.C. and Purrott, R.J. Radiation induced chromosome aberrations and the Poisson distribution. Rad. and Environm. Biophys., 16, 89-100 (1979).

[11] Roos, H. and Schmid, E. Analysis of chromosome aberrations in human peripheral lymphocytes induced by 5.4 keV x-rays., Radiat. Environ. Biophys., 36, 251-254 (1998).

[12] Norman, A. and Sasaki, M.S. Chromosome-exchange aberrations in human lymphocytes. Int. J. Rad. Biol., 11, 321-328 (1966).

Table 1 The relation between dose and chromosome aberrations (Sax, 1940) [8]

X-ray dose# (Gy)	Total chromosomes	Chromosome aberrations*				
		Dicentric	Ring	Total	%B	$(D/1.07)^2$
1	1800	5	1	6	0.7	0.8
2	1710	21	8	29	3.4	3.5
3	1464	48	13	61	8.3	7.8
4	1902	104	28	132	13.9	14.0
5	1530	134	25	159	20.8	21.8

* Each aberration involves two breaks. # Change the unit assumed as 100 r/Gy. B: Breaks, D: Dose.

Table 2 The relation between dose and one-hit and two-hit chromatid breaks [8]

X-ray dose# (Gy)	Total chromosomes	Chromatid breaks					
		1-Hit	%B	$(D/0.45)^{1.1}$	2-Hit	%B	$(D/0.67)^{1.9}$
0.1	6330	14	0.2	0.2	2	0.03	0.02
0.2	6930	24	0.4	0.5	4	0.06	0.08
0.4	8610	76	0.9	1.1	34	0.4	0.31
0.8	7368	148	2.0	1.9	112	1.5	1.4
1.2	4902	141	2.9	2.9	124	2.5	3.0
1.6	8292	375	4.4	4.0	422	5.1	5.3
2.0	8508	472	5.1	5.1	685	8.1	8.1

Change the unit assumed as 100 r/Gy. B: Breaks, D: Dose.

Table 3 Frequency of dicentrics after exposure of whole blood of healthy human *in vitro* (Vulpis, et al. 1976) [9]

X-ray dose (Gy)	Cells scored	Dicentrics	Dicentrics per cell #1	Statistical error #2
0	4336	0	0	0
0.05	4218	7	0.00166	0.00063
0.1	2996	18	0.00601	0.00141
0.2	3006	17	0.00566	0.00137
0.3	2196	40	0.01821	0.00285
0.4	2586	35	0.01353	0.00227
0.5	2736	83	0.03034	0.00328
0.6	1237	32	0.02587	0.00451
1	518	54	0.10425	0.01343
1.5	251	39	0.15538	0.02287
2	491	163	0.33198	0.02125
3	151	115	0.76159	0.03468
4	203	270	1.33005	0.08094

#1 values are recalculated.
#2 calculated by the binomial distribution (the largest data by Poisson distribution).

Table 4 Frequency of dicentrics observed in human lymphocytes irradiated by 250kVp X-rays at a dose-rate of 1 Gy/min (Edwards, et al. 1979) [10]

Dose (Gy)	Cells scored	Dicentrics	Dicentrics per cell	Statistical error #1
0.05	3325	9	0.00271	0.00090
0.1	4693	28	0.00597	0.00112
0.25	3547	49	0.01381	0.00196
0.50	2652	111	0.04186	0.00389
1	1869	200	0.10701	0.00715
2	266	99	0.37218	0.02964
2.5	183	100	0.54645	0.03680
3	293	219	0.74744	0.05051
4	247	323	1.30769	0.07276
6	100	224	2.24	0.14967
8	30	117	3.9	0.36056

#1 calculated by the binomial distribution (four largest data by Poisson distribution).

Table 5 Frequency of dicentrics observed in human lymphocytes irradiated by ^{60}Co gamma rays at a dose rate of 0.5 Gy/min (Edwards, et al. 1979) [10]

^{60}Co dose (Gy)	Cells scored	Dicentrics	Dicentrics per cell	Statistical error #1
0.25	6883	48	0.00697	0.00100
0.50	4917	119	0.02420	0.00219
1	2366	142	0.06002	0.00488
2	462	105	0.22727	0.01950
3	494	242	0.48988	0.02249
5	173	234	1.35260	0.08842
8	89	301	3.38202	0.19494

#1 calculated by the binomial distribution (two largest data by Poisson distribution).

Table 6 Frequency of dicentrics observed in human lymphocytes irradiated by 5.4 keV X-rays at a dose rate of 0.5 Gy/min (Roos and Schmid 1998) [11]

dose (Gy)	Cells scored	Dicentrics	Dicentrics per cell	Statistical error #1
0	35500	14	0.000394	0.00011
0.1	3000	30	0.01	0.00182
0.2	2000	41	0.0205	0.00317
0.5	500	39	0.078	0.01199
0.7	500	58	0.116	0.01432
1.0	500	95	0.19	0.01754
2.0	250	175	0.7	0.02898

#1 calculated by the binomial distribution.

Table 7 Frequency of dicentrics observed in human lymphocytes (Norman and Sasaki, 1966) [12]

X-ray dose (Gy)	Cells scored	Dicentrics	Dicentrics per cell #1	Statistical error #2
0.15	576	0	0.00	0.00
0.50	800	9	0.01125	0.00375
1	270	13	0.04815	0.01335
1.5	250	29	0.11600	0.02154
2	150	25	0.16667	0.03333
3	100	49	0.49000	0.07000
4	160	117	0.73125	0.06760
5	200	261	1.30500	0.08078
6	150	234	1.56000	0.10198
8	120	307	2.55833	0.14601
12	130	609	4.68462	0.18983
20	120	1007	8.39167	0.26444
25	60	593	9.88333	0.40586
30	62	688	11.09677	0.42306

#1 calculated by us. #2 calculated by Poisson distribution.

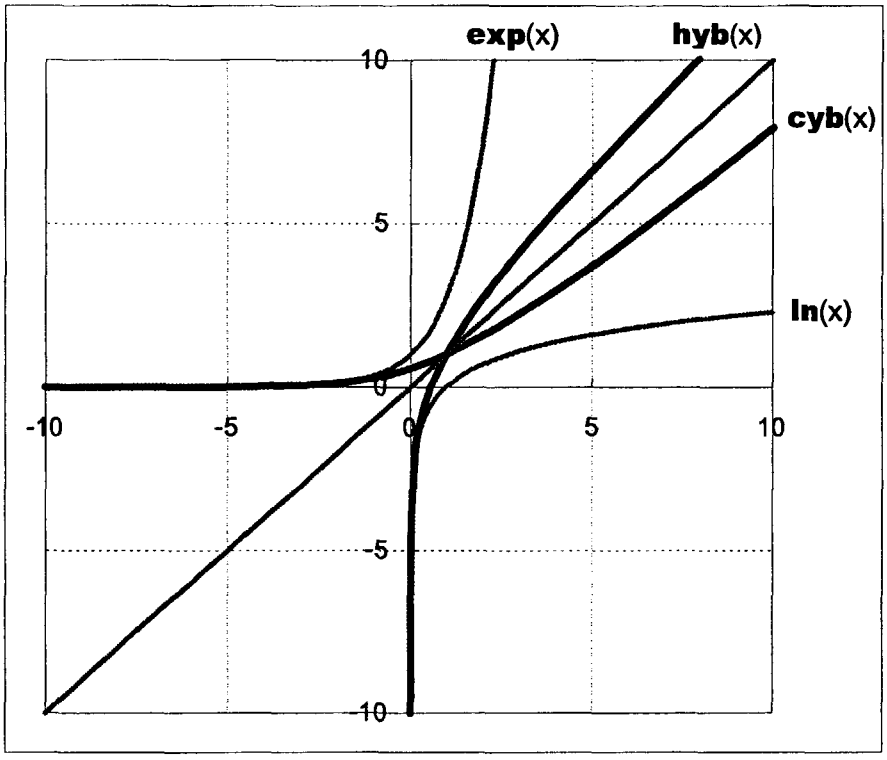

Figure 1 Graphs of the hybrid function, hyb(x), and its inverse function, cyb(x), corresponding to the logarithmic function, ln(x), and its inverse function (the exponential function), exp(x), respectively.

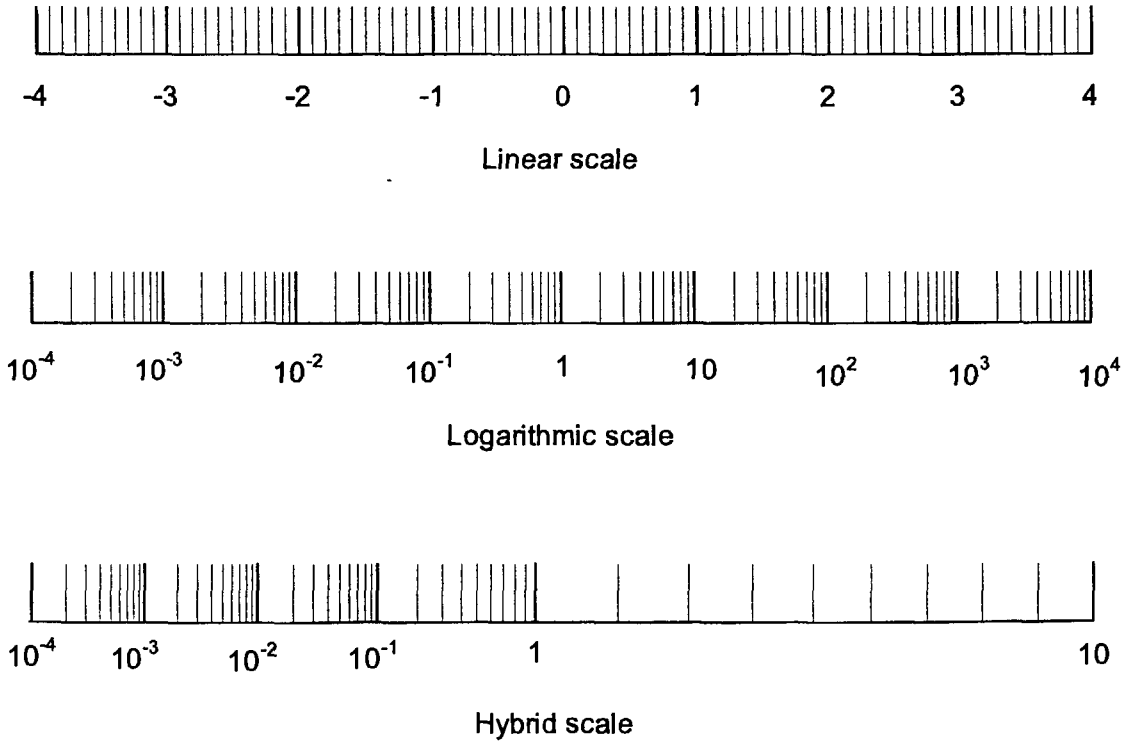

Figure 2 An example of the hybrid scale, which unifies the linear and the logarithmic scales.

x-axis → / ↓ y-axis	Logarithmic	Hybrid	Linear
Linear	Semi-Log	Semi-Hybrid	Linear-Linear
Hybrid	Log-Hybrid	Hybrid-Hybrid	Semi-Hybrid
Logarithmic	Log-Log	Log-Hybrid	Semi-Log

Figure 3 Nine types of section papers derived from introducing the hybrid scale.

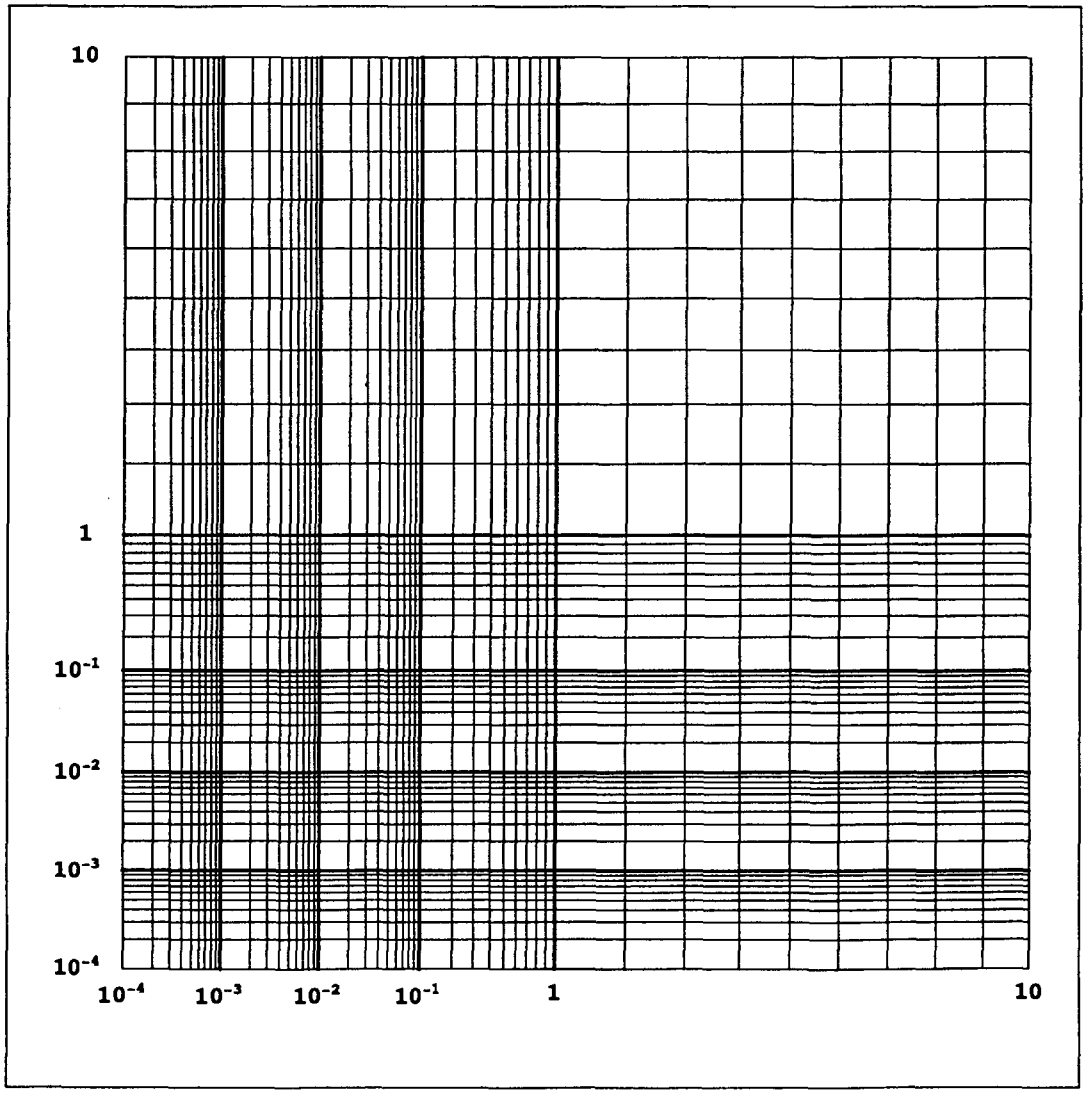

Figure 4 Hybrid-hybrid section paper.

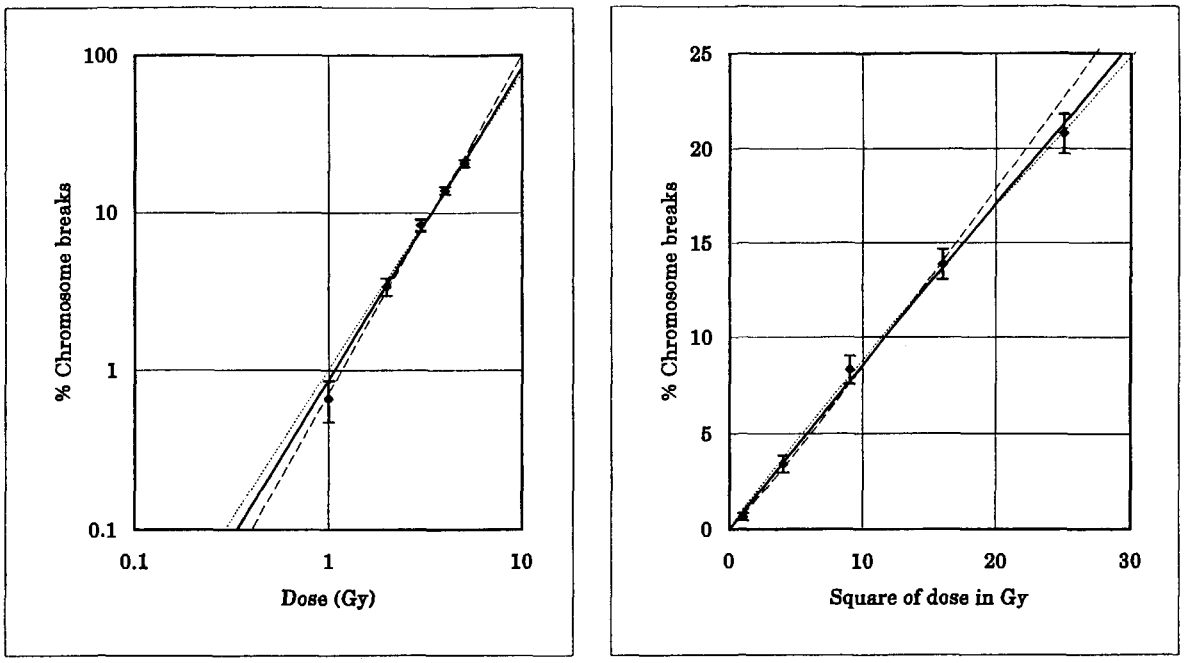

Figure 5 Percent chromosome breaks (Table 1) plotted on the log-log (left panel) and the quadratic-linear (right panel). Solid line: fitted by the power function model on the log scale, weighted by statistical errors (see error bars). Broken line: the same but without weight. Dotted line: fitted by the same model on the linear scale without weight.

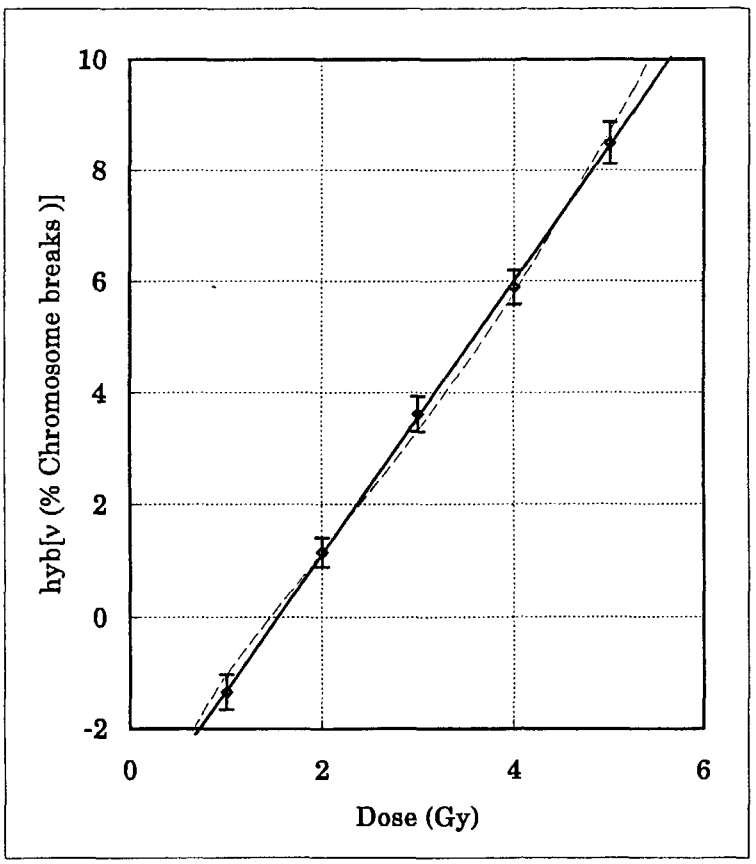

Figure 6 Plots of the same chromosome breaks on the hybrid scale, where ν=0.318. Broken line: best fit of the quadratic model to the data on the hybrid scale. Solid line: best fit of a straight line to the data on the hybrid scale, which represents the fourth HS model.

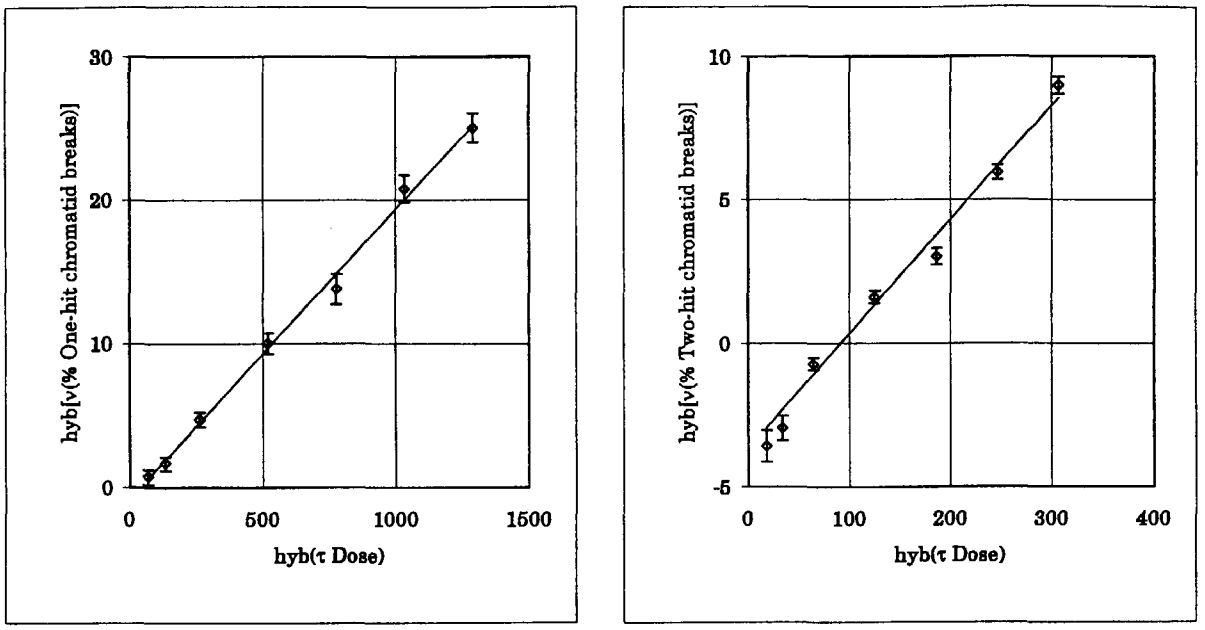

Figure 7 Percent chromatid breaks of one-hit (left panel) and two-hit (right panel), in Table 2, plotted on the hybrid-hybrid paper. The error bar represents the statistical error. The straight line of each panel is the best fit to the data on the hybrid-hybrid paper.

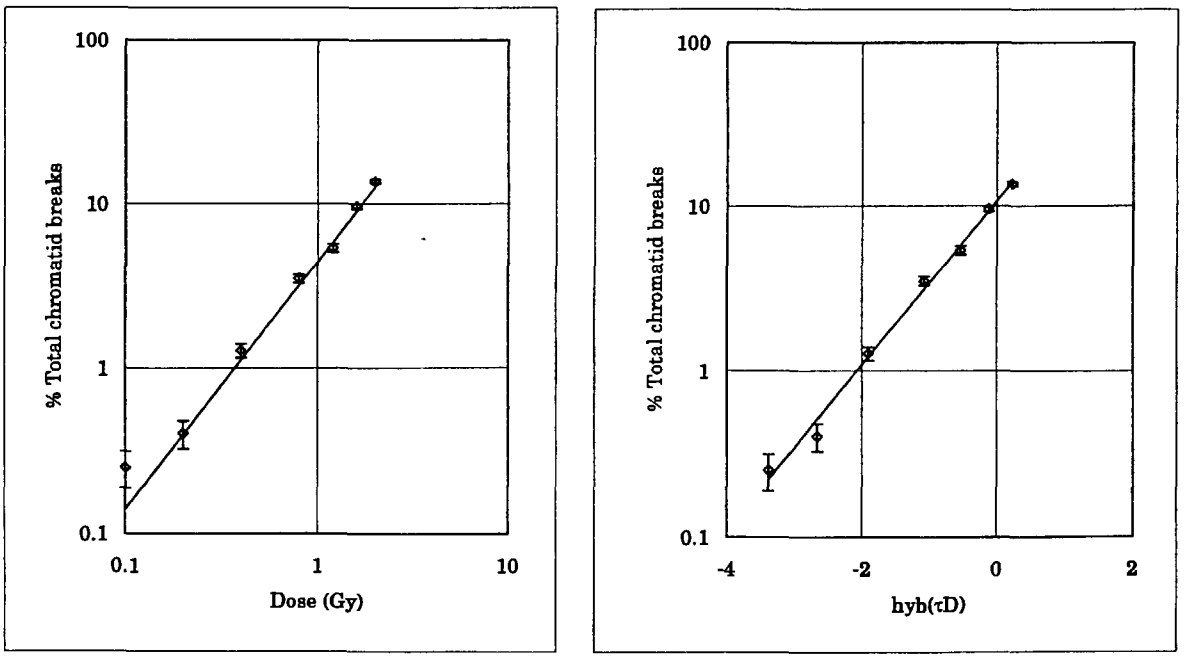

Figure 8 Total percent chromatid breaks (sum of one-hit and two-hit) plotted on the log-log paper (left panel) and on the hybrid-log paper (right panel). A straight line on left panel represents the power function model and that on right panel the second HS model. The error bar represents the statistical error.

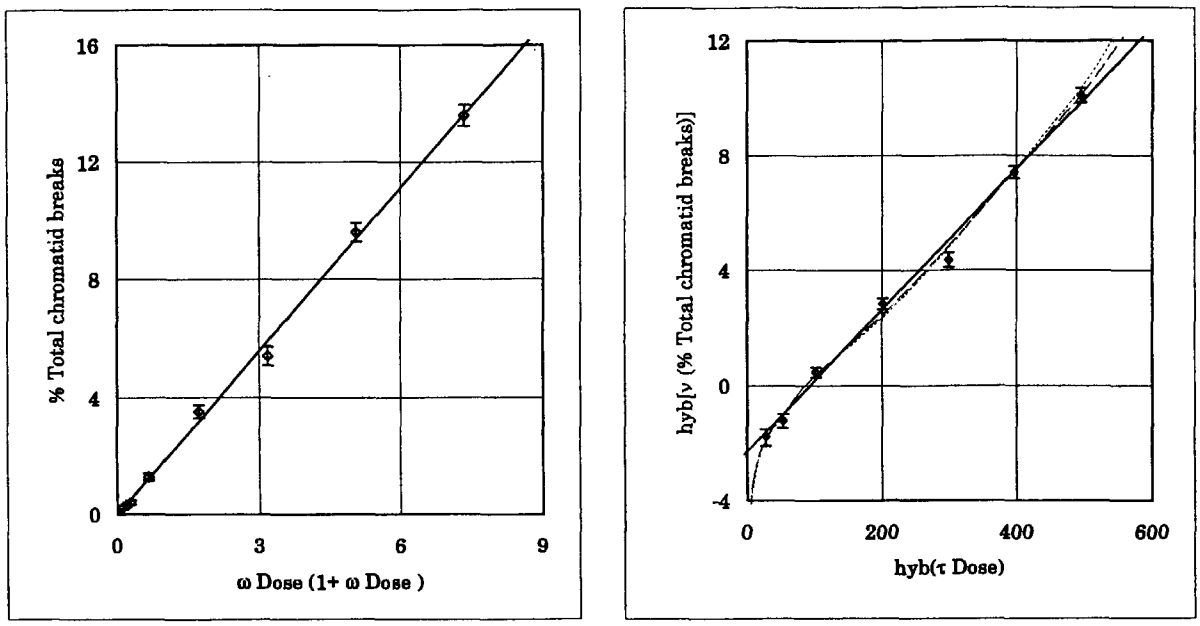

Figure 9 The same total chromatid breaks as Figure 9, applied to the linear-quadratic model (left panel) and the hybrid-hybrid model (right panel). A straight line on each panel represents each model, respectively. On right panel, the dotted curve represents the second HS model, and the broken curve the linear-quadratic model.

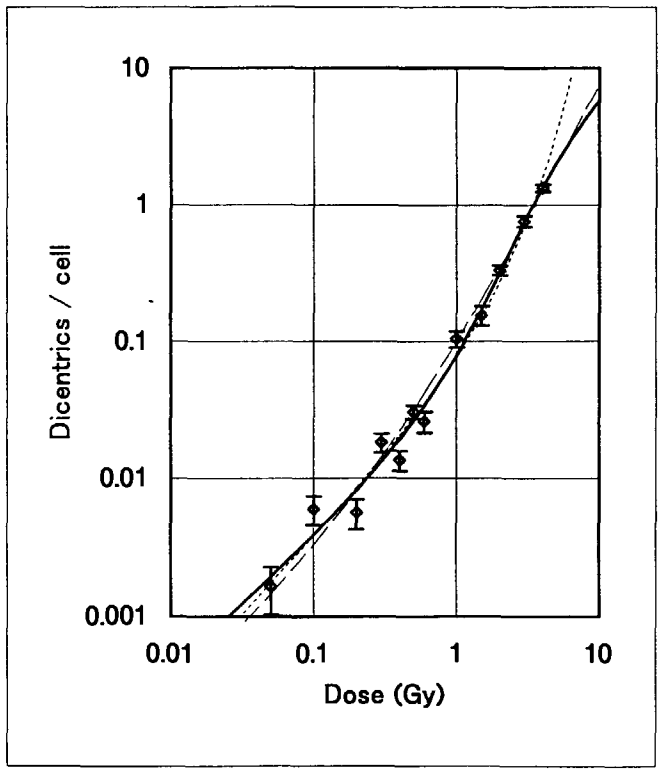

Figure 10 Dicentrics per human cell irradiated by X-ray (see Table 3, Vulpis, et al., 1976), plotted on the log-log paper with the bar of statistical error. The broken line represents the L-Q model fitted to the data on the hybrid scale of hyb(1.28Yield), the dotted line the second HS model, and the solid line the hybrid-hybrid model.

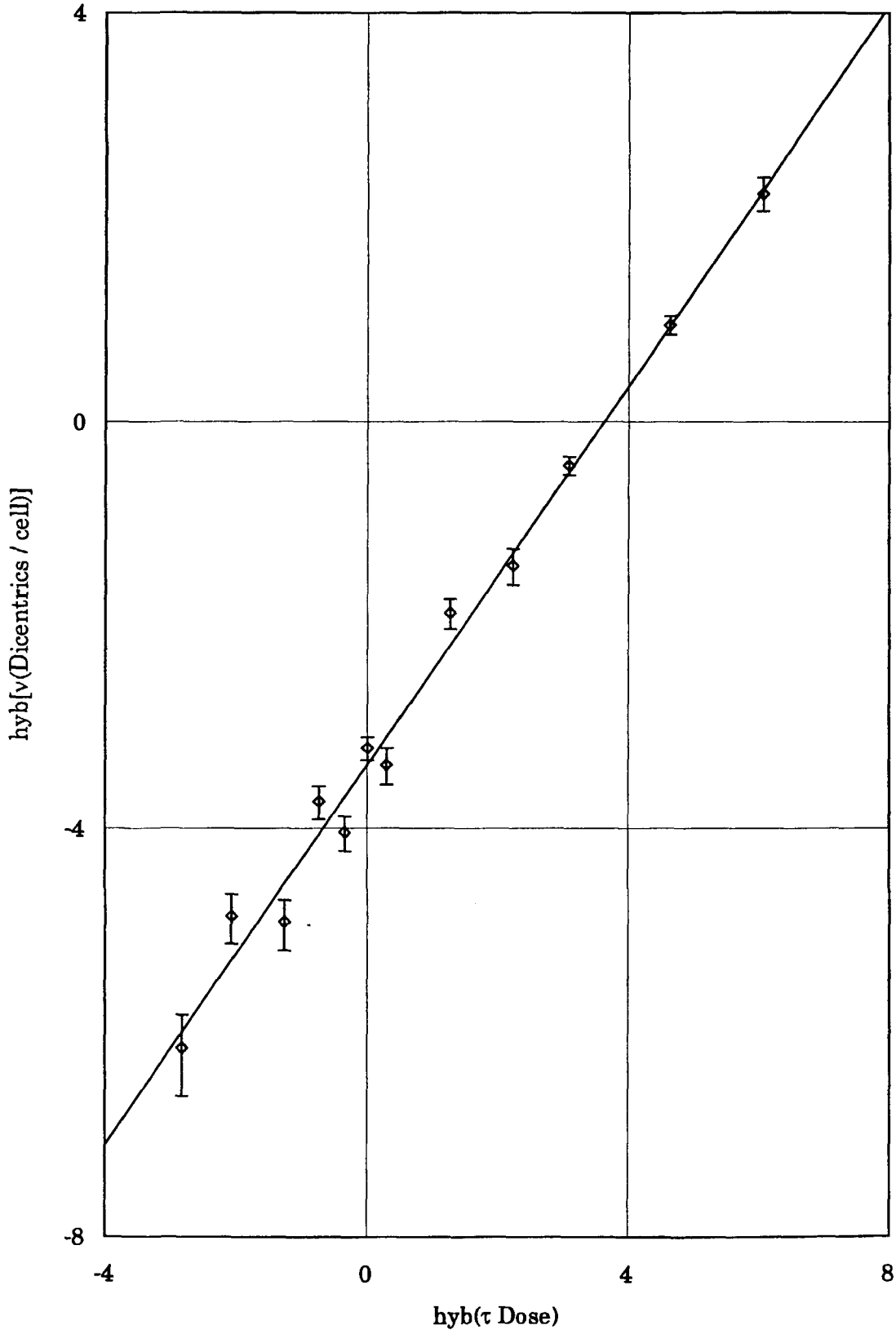

Figure 11 Best-fit straight line of the calibration curve to the data of Vulpis, et al. (1976), shown in Table 3, estimated by the hybrid-hybrid model. Error bars: statistical errors.

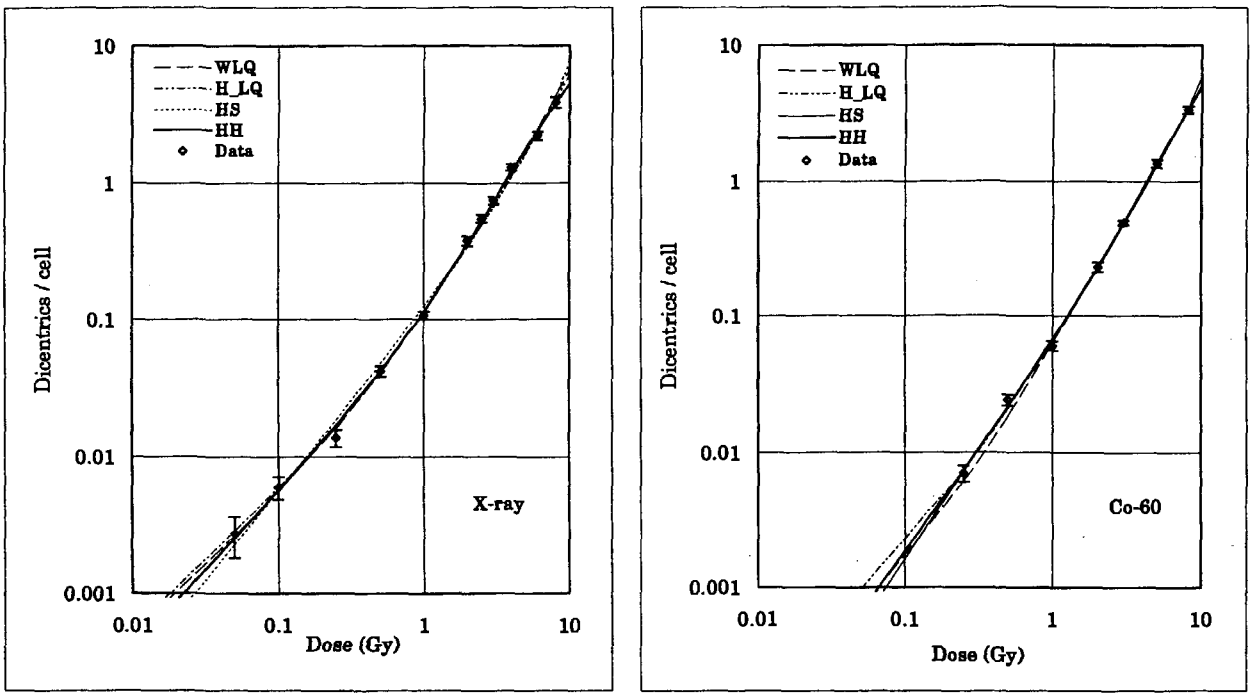

Figure 12 Dicentrics per cell induced by X-ray (left panel) and cobalt-60 (right panel), shown in Table 4 (Edwards, et al. 1979), plotted on the log-log paper. WLQ is the weighted L-Q model, H_LQ is the hybrid-scaled L-Q model, HS is the second HS model, and HH is the hybrid-hybrid model. The error bar represents the statistical error.

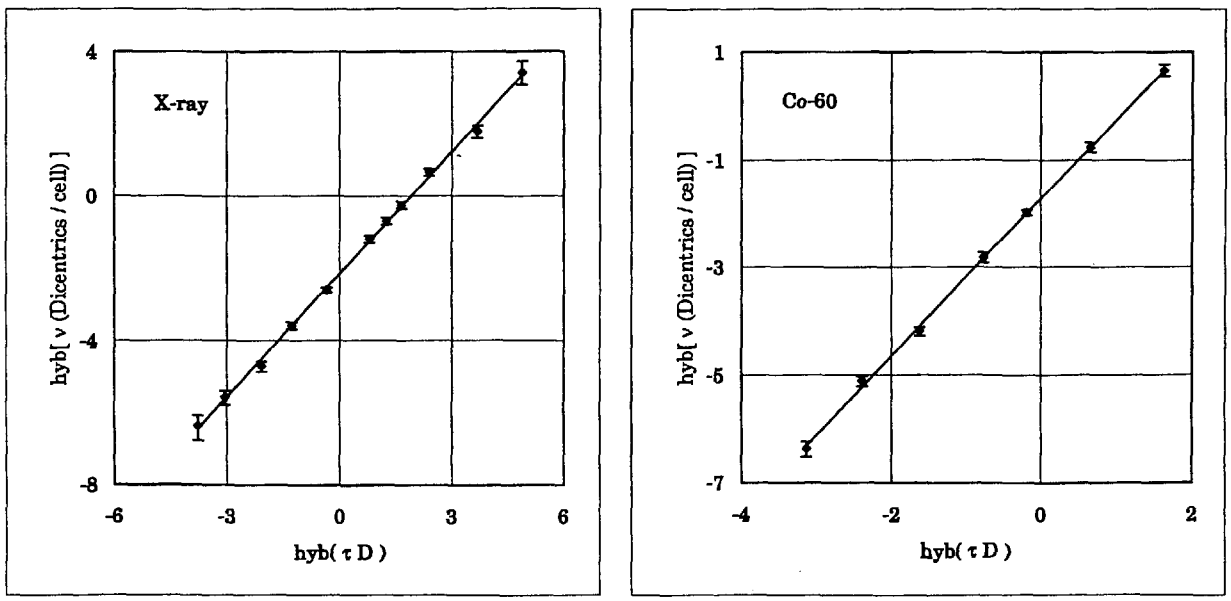

Figure 13 Best-fit straight lines of the calibration curves to X-ray (left panel) and cobalt-60 (right panel) data of Edwards, et al.(1979), estimated by the hybrid-hybrid model. The error bar represents the statistical error.

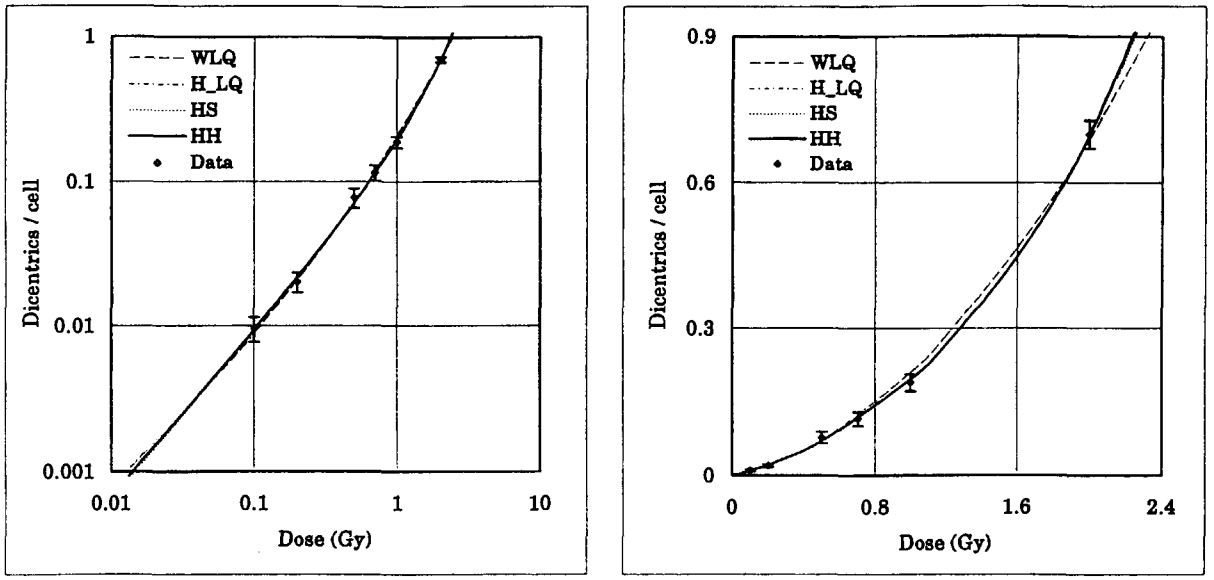

Figure 14 Dicentrics per cell induced by 5.4 keV X-ray in Table 6 (Roos and Schmid 1979), plotted on the log-log (left panel) and normal section paper (right panel),. WLQ is the weighted L-Q model, H_LQ is the hybrid-scaled L-Q model, HS is the second HS model, and HH is the hybrid-hybrid model. The error bar: the statistical error.

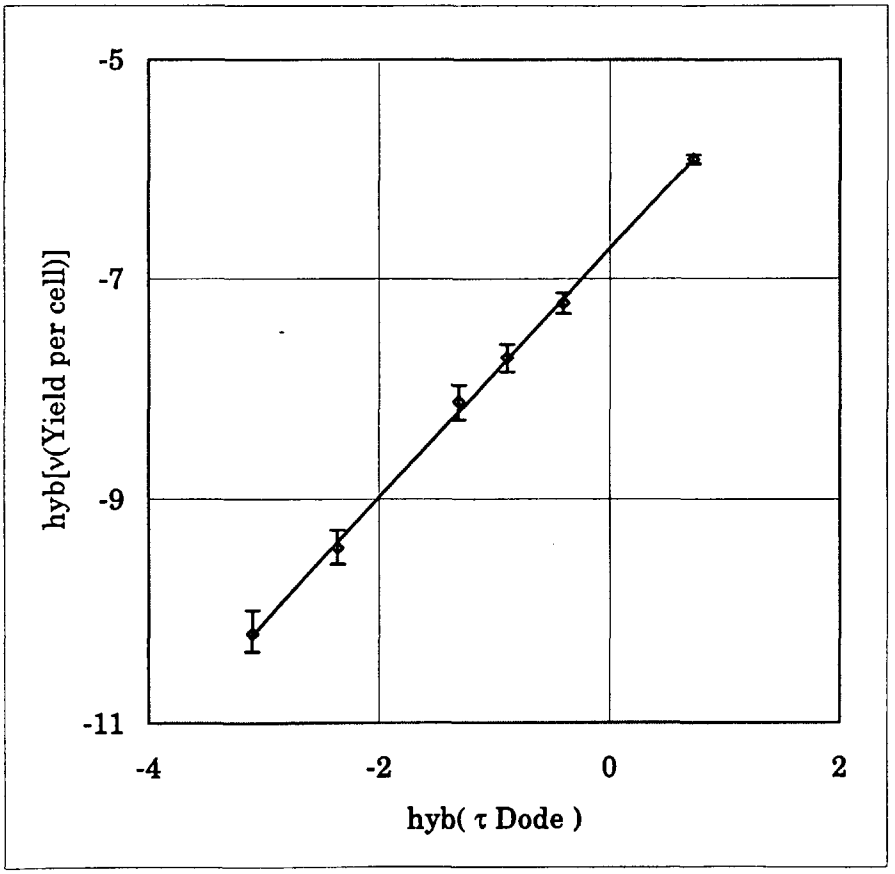

Figure 15 Best-fit straight line of the calibration curves to the data of Roos and Schmit (1998), estimated by the hybrid-hybrid model. The error bar represents the statistical error.

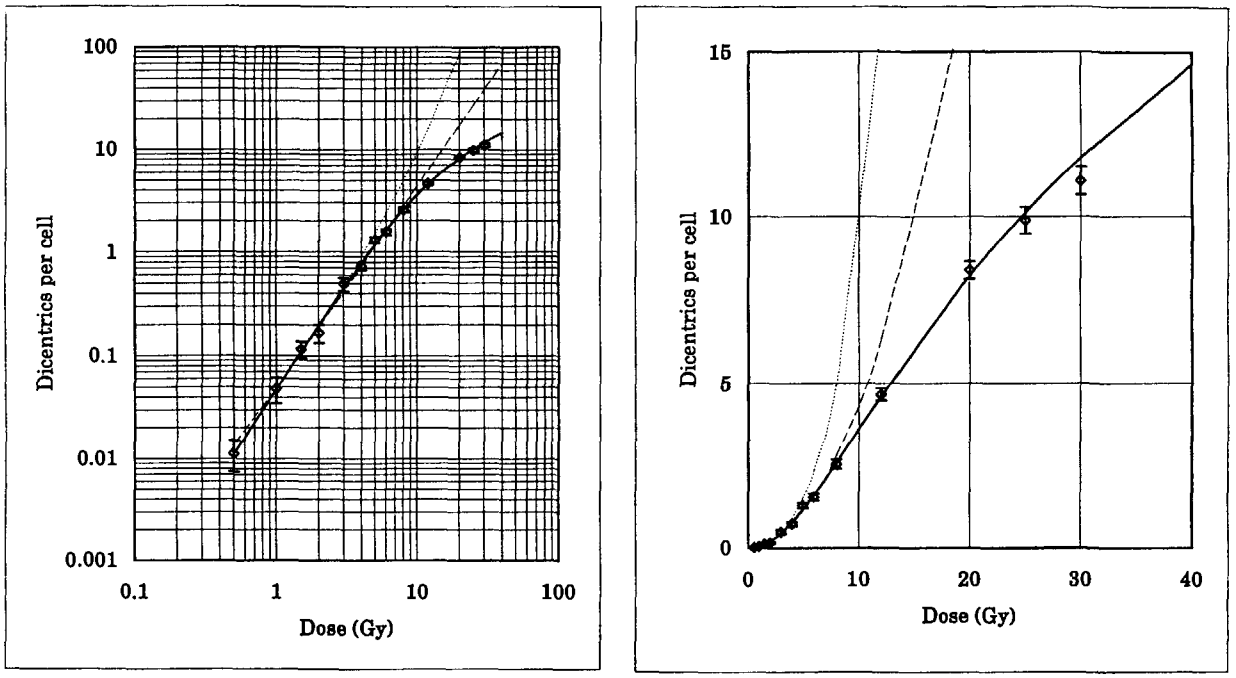

Figure 16 Dicentrics per cell induced by X-ray with the mean energy of 1.9MeV, shown in Table 7 (Norman and Sasaki 1966), plotted on the log-log paper (left panel) and the normal section paper (right panel). Broken line represents the best fit of the weighted L-Q model, dotted line that of the second HS model and solid line that of the hybrid-hybrid model. The error bar represents the statistical error.

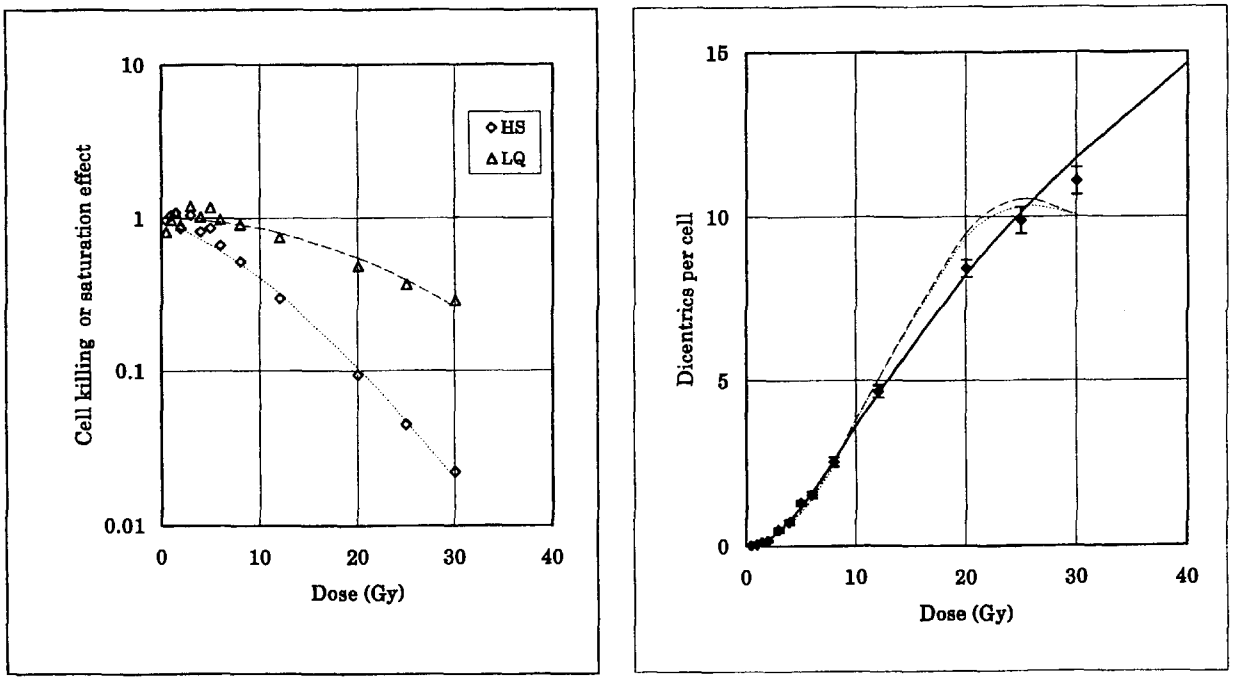

Figure 17 Surviving fractions (left panel) calculated by the weighted L-Q and the second HS models, and their corresponding dose-response curves (right panel). Broken line: weighted L-Q model. Dotted line: second HS model. Solid line: HH model.

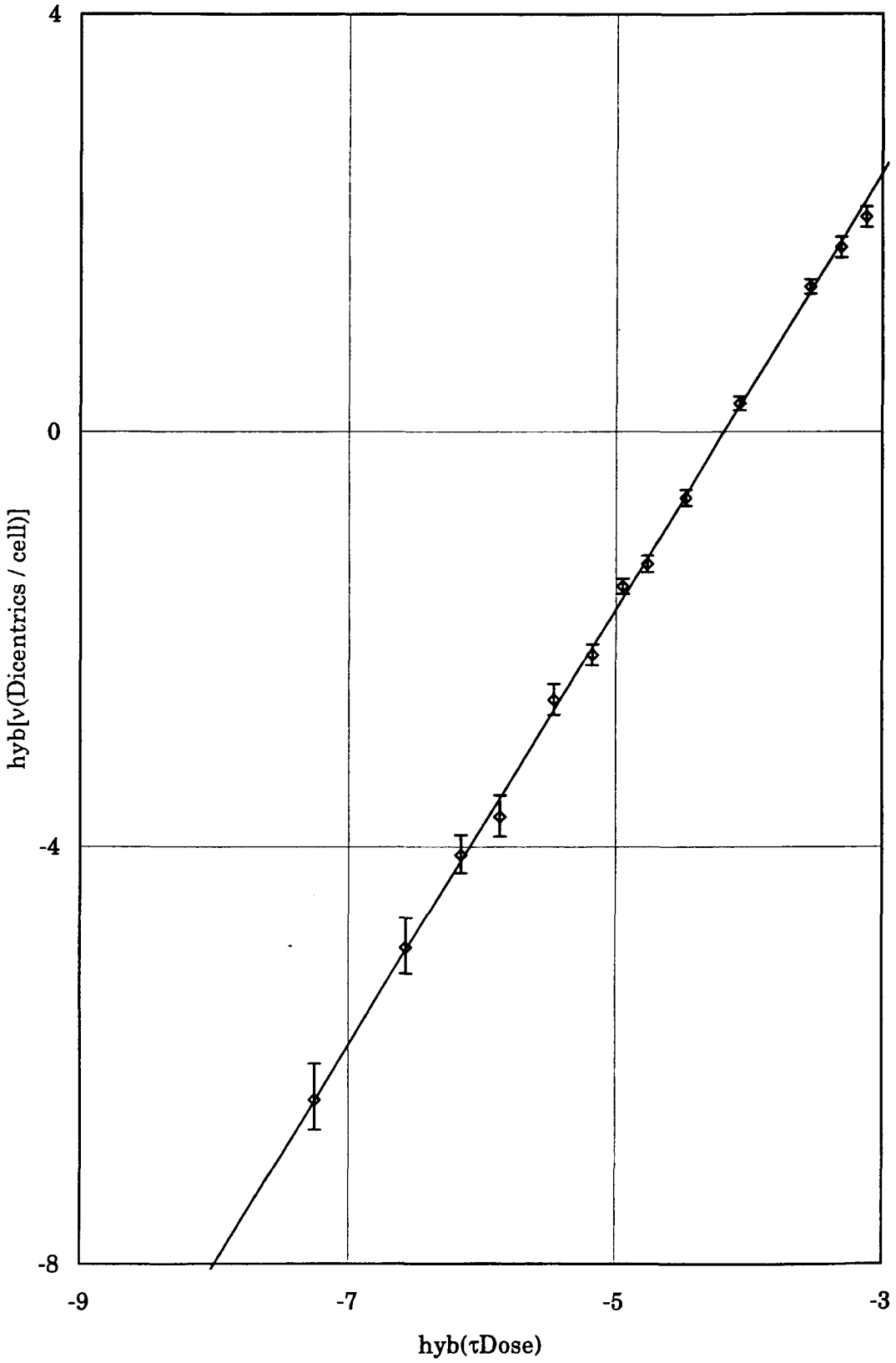

Figure 18 Best-fit straight line of the calibration curve to the data of Norman and Sasaki (1966), shown in Table 7, estimated by the hybrid-hybrid model. Error bars: statistical errors.

国際単位系(SI)と換算表

表1　SI基本単位および補助単位

量	名称	記号
長さ	メートル	m
質量	キログラム	kg
時間	秒	s
電流	アンペア	A
熱力学温度	ケルビン	K
物質量	モル	mol
光度	カンデラ	cd
平面角	ラジアン	rad
立体角	ステラジアン	sr

表2　SIと併用される単位

名称	記号
分，時，日	min，h，d
度，分，秒	°，′，″
リットル	l，L
トン	t
電子ボルト	eV
原子質量単位	u

1 eV = 1.60218 × 10^{-19} J

1 u = 1.66054 × 10^{-27} kg

表5　SI接頭語

倍数	接頭語	記号
10^{18}	エクサ	E
10^{15}	ペタ	P
10^{12}	テラ	T
10^{9}	ギガ	G
10^{6}	メガ	M
10^{3}	キロ	k
10^{2}	ヘクト	h
10^{1}	デカ	da
10^{-1}	デシ	d
10^{-2}	センチ	c
10^{-3}	ミリ	m
10^{-6}	マイクロ	μ
10^{-9}	ナノ	n
10^{-12}	ピコ	p
10^{-15}	フェムト	f
10^{-18}	アト	a

表3　固有の名称をもつSI組立単位

量	名称	記号	他のSI単位による表現
周波数	ヘルツ	Hz	s^{-1}
力	ニュートン	N	$m \cdot kg/s^2$
圧力，応力	パスカル	Pa	N/m^2
エネルギー，仕事，熱量	ジュール	J	N·m
工率，放射束	ワット	W	J/s
電気量，電荷	クーロン	C	A·s
電位，電圧，起電力	ボルト	V	W/A
静電容量	ファラド	F	C/V
電気抵抗	オーム	Ω	V/A
コンダクタンス	ジーメンス	S	A/V
磁束	ウェーバ	Wb	V·s
磁束密度	テスラ	T	Wb/m^2
インダクタンス	ヘンリー	H	Wb/A
セルシウス温度	セルシウス度	℃	
光束	ルーメン	lm	cd·sr
照度	ルクス	lx	lm/m^2
放射能	ベクレル	Bq	s^{-1}
吸収線量	グレイ	Gy	J/kg
線量当量	シーベルト	Sv	J/kg

表4　SIと共に暫定的に維持される単位

名称	記号
オングストローム	Å
バーン	b
バール	bar
ガル	Gal
キュリー	Ci
レントゲン	R
ラド	rad
レム	rem

1 Å = 0.1 nm = 10^{-10} m

1 b = 100 fm^2 = 10^{-28} m^2

1 bar = 0.1 MPa = 10^5 Pa

1 Gal = 1 cm/s^2 = 10^{-2} m/s^2

1 Ci = 3.7 × 10^{10} Bq

1 R = 2.58 × 10^{-4} C/kg

1 rad = 1 cGy = 10^{-2} Gy

1 rem = 1 cSv = 10^{-2} Sv

（注）

1. 表1－5は「国際単位系」第5版，国際度量衡局 1985年刊行による。ただし，1 eVおよび1 uの値はCODATAの1986年推奨値によった。
2. 表4には海里，ノット，アール，ヘクタールも含まれているが日常の単位なのでここでは省略した。
3. barは，JISでは流体の圧力を表わす場合に限り表2のカテゴリーに分類されている。
4. EC閣僚理事会指令ではbar，barnおよび「血圧の単位」mmHgを表2のカテゴリーに入れている。

換算表

力	N(=10^5 dyn)	kgf	lbf
	1	0.101972	0.224809
	9.80665	1	2.20462
	4.44822	0.453592	1

粘度　1 Pa·s(N·s/m^2) = 10 P(ポアズ)(g/(cm·s))

動粘度　1 m^2/s = 10^4 St(ストークス)(cm^2/s)

圧力	MPa(=10 bar)	kgf/cm^2	atm	mmHg(Torr)	lbf/in^2(psi)
	1	10.1972	9.86923	7.50062 × 10^3	145.038
	0.0980665	1	0.967841	735.559	14.2233
	0.101325	1.03323	1	760	14.6959
	1.33322 × 10^{-4}	1.35951 × 10^{-3}	1.31579 × 10^{-3}	1	1.93368 × 10^{-2}
	6.89476 × 10^{-3}	7.03070 × 10^{-2}	6.80460 × 10^{-2}	51.7149	1

エネルギー・仕事・熱量	J(=10^7 erg)	kgf·m	kW·h	cal(計量法)	Btu	ft·lbf	eV
	1	0.101972	2.77778 × 10^{-7}	0.238889	9.47813 × 10^{-4}	0.737562	6.24150 × 10^{18}
	9.80665	1	2.72407 × 10^{-6}	2.34270	9.29487 × 10^{-3}	7.23301	6.12082 × 10^{19}
	3.6 × 10^6	3.67098 × 10^5	1	8.59999 × 10^5	3412.13	2.65522 × 10^6	2.24694 × 10^{25}
	4.18605	0.426858	1.16279 × 10^{-6}	1	3.96759 × 10^{-3}	3.08747	2.61272 × 10^{19}
	1055.06	107.586	2.93072 × 10^{-4}	252.042	1	778.172	6.58515 × 10^{21}
	1.35582	0.138255	3.76616 × 10^{-7}	0.323890	1.28506 × 10^{-3}	1	8.46233 × 10^{18}
	1.60218 × 10^{-19}	1.63377 × 10^{-20}	4.45050 × 10^{-26}	3.82743 × 10^{-20}	1.51857 × 10^{-22}	1.18171 × 10^{-19}	1

1 cal = 4.18605 J（計量法）

= 4.184 J　（熱化学）

= 4.1855 J（15 °C）

= 4.1868 J（国際蒸気表）

仕事率　1 PS（仏馬力）

= 75 kgf·m/s

= 735.499 W

放射能	Bq	Ci
	1	2.70270 × 10^{-11}
	3.7 × 10^{10}	1

吸収線量	Gy	rad
	1	100
	0.01	1

照射線量	C/kg	R
	1	3876
	2.58 × 10^{-4}	1

線量当量	Sv	rem
	1	100
	0.01	1

（86年12月26日現在）